# AN IMPEDANCE CARDIOGRAPH

A dissertation
submitted in partial fulfillment of the requirements
for the degree of
**Master of Technology**

By
**Babu P. Kuriakose**
(Roll No: 98314301)
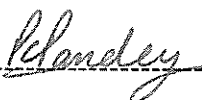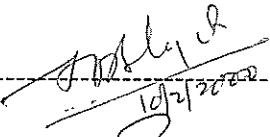
Guide
Prof. P.C. Pandey

School of Biomedical Engineering
Indian Institute of Technology, Bombay

January 2000

# Indian Institute of Technology, Bombay

## Dissertation Approval

The dissertation entitled "An impedance cardiograph", by Shri Babu P.Kuriakose

(Roll. No. 98314301) is approved for award of the degree of **Master of Technology** in

Biomedical Engineering.


Supervisor —————— *[signature]* ————— (Prof. P.C.Pandey)


External examiner ————— *[signature]* ————— (Prof. S.D.Bhagwat)


Internal examiner ————————————————— (Prof. S.Mukherji)


Chairperson ————— *[signature]* ————— (Prof. S.Chaudhuri)


Date : 10th February, 2000

# CONTENTS

# CONTENTS

# CONTENTS

**Babu P. Kuriakose :** *An Impedance Cardiograph*, M Tech. dissertation, School of Biomedical Engineering, IIT Bombay, January 2000, Guide: Dr. P.C. Pandey.

===========================================================================

# ABSTRACT

Impedance cardiography (ICG) is a non-invasive technique for measuring the impedance variation in the human thorax according to the changes in blood volume. This technique is used for estimation of cardiac output and diagnosis of cardiac disorders. The aim of this project is to develop an impedance cardiograph instrument. The instrument hardware extracts the physiological signal namely impedance signal $z(t)$, its derivative $dz(t)/dt$ , basal impedance $Z_0$ and differentiated electrocardiogram $d(ECG)/dt$. To calibrate the ICG instrument, a thoracic impedance simulator has also been developed.

The work involved the testing and modification of circuits developed for ICG instrument, and development and implementation of a thoracic impedance simulator. Each instrument has been assembled as a single PCB and housed in a cabinet, with all the appropriate connectors and controls.

*Pandey* 11·2·00

# ACKNOWLEDGEMENT

I thank my guide, Prof. P.C. Pandey, for his valuable guidance and immense help in completion of this project. I am thankful to all friends in the laboratory for their valuable assistance.

IIT Bombay

January 2000                                                          Babu P. Kuriakose

ii

# List of Abbreviations

| Abbreviation | Term |
| --- | --- |
| AV | atrio-ventricular |
| CO | cardiac output |
| CMRR | common-mode rejection ratio |
| DAQ | data acquisition card |
| ECG | electrocardiogram |
| HR | heart rate |
| ICG | impedance cardiogram |
| PC | personnel computer |
| PCMCIA | Personnel Computer Memory Card Interface Association |
| PCB | printed circuit board |
| PCG | phonocardiogram |
| SA | sino-atrial |
| V/I | voltage-to-current |

# List of Symbols

| Symbols | Explanation |
|---|---|
| $L$ | length of the thorax under measurement |
| $Z_0$ | basal impedance |
| $Z_t$ | total impedance change |
| $v$ | changing volume |
| $\Delta V$ | maximum change in volume |
| $\Delta Z$ | maximum change in impedance |
| $Z_n$ | impedance of changing volume |
| $z$ | small change in impedance |
| $\rho$ | resistivity of blood |
| $T_{lvet}$ | left ventricular ejection time |
| $z(t)$ | instantaneous change in impedance |
| $dz(t)/dt_{max}$ | maximum value of derivative of $z$ w.r.t time |
| $d(ECG)/dt$ | first derivative of ECG w.r.t time |
| $f_T$ | unity-gain bandwidth product |
| $\Delta R$ | change in resistance |

## List of Figures

## List of Figures

# Chapter 1

# Introduction

## 1.1 Overview

In general, the human body may be treated as an ionic conductor, and blood is a good conductor of electricity compared to tissues. The decrease in electrical impedance occurs, when a volume of blood is introduced between any body segment under measurement. Impedance cardiography (ICG) is a technique for recording the impedance variations in the thorax during heartbeats. Using this technique, stroke volume and hence cardiac output can be measured. Stroke volume is the amount of blood pumped out from heart during a cardiac cycle. Cardiac output is the volume of blood pumped out in one minute expressed in liters/minute. Several invasive instruments for this purpose have already been developed and their use is quite common in hospitals. However, an instrument based on impedance cardiography are at present not in clinical use.

## 1.2 Project Objective

The aim of this project is to develop the hardware of an impedance cardiography system. This system involves a battery operated ICG instrument that can be interfaced to a data acquisition card of a computer for signal acquisition and processing. ICG instrument consists of a constant current source for a high frequency signal injection to the thorax region, impedance detector and signal conditioning hardware. The system has to monitor the heartbeat, stroke volume and cardiac output. A thorax impedance simulator system is also implemented, which will be helpful for testing and calibration of the instrument. This project is a continuation of earlier work carried out at IIT Bombay, and involves modifications and redesign of the hardware to improve the sensitivity and consistency of the instrument.

1

## 1.3 Outline

The fundamentals of impedance cardiography are given in second chapter. Chapter 3 gives a description of ICG and ECG extraction circuit of the instrument developed earlier. Chapter 4 describes the development work done, i.e., modifications in the hardware of the ICG instrument and thoracic impedance simulator. Chapter 5 presents circuit assembly and test results of various stages in the hardware. Chapter 6 gives the summary and conclusions.

## Chapter 2

# Fundamentals of Impedance Cardiography

## 2.1 Introduction

The first section of this chapter explains the anatomy and functioning of human heart, electrical activity for heart beats and cardiac cycle. The second section explains the impedance variations in thorax region associated with the blood pumped from the heart. The relationship between the blood volume change and impedance change formulated in this section. The expression for finding stroke volume from the above relationship is also given. The last section of this chapter explains the electrical analogy of thorax and impedance measurement technique.

## 2.2 The Human Heart

### 2.2.1 Anatomy and functioning of heart

The physical structure of the heart is shown in Fig 2.1. It has four separate pumps; two primer pumps, the atria and two power pumps, the ventricles. The period from the end of one heart contraction to the end of the next is called the cardiac cycle. The right heart pumps the blood through the lungs and left heart pumps the blood through the peripheral organs. The basic pulmonary circulation and systemic circulation is shown in Fig 2.2. Atrium is the entryway of blood to the ventricle. The blood is pumped to the ventricle and then propels to the pulmonary or peripheral circulation with a large force. Special mechanisms in the heart maintain cardiac rhythmicity and transmit action potentials throughout the heart muscle to cause heart's rhythmical beat [1][2]. The pumping activity of the heart is so regulated that the heart can pump either small or large amount of blood as dictated by the needs of the body. The left ventricle is important of all chambers, which pumps the blood to the entire body. The pumping action takes place when the left ventricle contracts and blood is supplied to the body through the aorta.

The heartbeats are initiated in the heart itself from electrical impulses generated by sino-atrial (SA) and atrio-ventricular (AV) node in a particular rhythm [1]. These impulses are conducted through the cardiac muscles to all parts of the heart. The contraction and relaxation of all chambers are synchronized with this electrical activity of the heart. These impulses give rise to weak currents on the surface of the skin. The resulting potential differences between standardized sites on the skin are measured using surface electrodes and these signals are called electrocardiogram (ECG) waveforms. The electrocardiogram is composed of both depolarization and repolarization waves passing through the heart muscles. The contraction and relaxation of atria and ventricles occur according to the depolarization and repolarization activities of heart cells. Valves associated with the chambers regulate the pumping action of heart.

During the opening and closure of valves, vibrations are generated. When the valves close, the vanes of the valves and surrounding fluids vibrate under the sudden pressure change, giving off sound that travels through the chest. When the ventricles first contract, vibrations are generated by the closure of AV valves. This is a low pitch vibration and of a relatively long period, called as first heart sound. When the aortic and pulmonary valves close with a relatively rapid snap, the vibrations are short period, called as second heart sound [1]. These vibrations are picked using a microphone and the processed signal is called phonocardiogram (PCG).

## 2.2.2 The cardiac cycle

The cardiac cycle consists of a period of relaxation called diastole followed by a period of contraction called systole. Each cycle is initiated by spontaneous generation of an action potential in the SA node located in the anterior wall of the right atrium near the opening of the superior vena cava. The action potentials travel rapidly through both atria and thence through AV bundle into the ventricles. There is a delay of 100 ms between the passage of cardiac impulse from atria to the ventricle. This allows the atria to contract ahead of the ventricles, thereby pumping blood into the ventricles prior to the very strong

4

ventricular contraction. The different events in the cardiac cycle are shown in Fig 2.3. These curves show the pressure changes in the aorta, left ventricle and the left atrium.

The *a* wave is caused by atrial contraction, has a very low pressure rises about 7-8 mmHg. At the end of the *a* wave, ventricular contraction starts. Now AV valve is closed. Immediately after ventricular contraction begins, the ventricular pressure abruptly rises. The time required for building up of sufficient pressure is around 20-30 milliseconds. This pushes the aortic and pulmonary valves open. Immediately blood begins to pour out of the ventricles, with about 70 percent of the emptying occurring during the first one-third period of ejection. The first period is called rapid ejection and second is slow ejection period [1]. At the end of systole, ventricular relaxation begins suddenly, falling the intraventricular pressure rapidly. Then the AV valve opens and rapid filling phase of ventricle starts. This begins to a new cardiac cycle. The volume of blood pumped by the heart into the aorta during one cardiac cycle is known as stroke volume (SV). The total volume of blood pumped by the heart in one minute is called cardiac output. For a normal human being, the total blood volume in each ventricle is about 120 to 130 ml. The stroke volume is 70 ml and cardiac output is around 5 liters [1].

## 2.3 Basis for Impedance Cardiography

Biological tissue consists of an aggregation of cells of differing shapes bonded together and surrounded by tissue fluids, which are electrolytes. The current injected into the tissue under study can pass around the cells as well as through the cells. If the injected current is dc or very slow varying, it flows through the electrolytes. Therefore low frequency impedance is high. The impedance decreases with increase in frequency, due to decrease in reactance of the cell wall capacitance, and the current flows through the cytoplasm as well as through the electrolytes [3]. For frequency above 20 kHz the reactance of cell wall becomes negligible and the impedance becomes resistive. At frequencies above about 1 MHz, the excitation current remains confined to the chest wall, and the impedance is not affected by the blood volume changes. Therefore impedance cardiography generally employ excitation in the range of 40 kHz – 500 kHz. The

5

biological tissue is not generally excitable in this range. Threshold of perception in this region is in tens of mA, and therefore excitation current can be safely used up to 10 mA. Table 1 shows the resistivities measured for biomaterials at 100 kHz [4]. This shows blood is the least resistive material in human body and has major influence for impedance variation.

In impedance plethysmography, an alternating current within the safe limits, is passed longitudinally across the body segment. Voltage between the two sensing electrodes is the current multiplied by the impedance in the current path. These changes in voltages are picked up and processed. The small voltage change sensed across the thoracic region is mainly due to the changes in blood volume in the heart. The volume of tissues, muscles, bones etc. remains the same, hence their contribution to the impedance signal is constant. When blood is pumped into the lungs during systole, the thoracic impedance decreases due to increased blood volume. This decrease in impedance is of the order of $0.1\ \Omega$ to $0.22\ \Omega$ [5]. It is detected and processed for getting impedance cardiogram.

## 2.4 Impedance model of thorax

The model used to quantify the thoracic impedance change is known as the parallel column model, shown in Fig 2.4. It consists of a column M of conducting material with constant impedance $Z_0$, in parallel with another column N having uniform cross sectional area and impedance $Z_n$

The net impedance is given as

$$Z(t) = Z_0 \parallel Z_n \tag{1}$$

The uniform cross sectional area A of cylinder N changes from zero to a final value; and results in a small change in the impedance measurement across the parallel columns.

$$z(t) = Z(t) - Z_0$$

$$= -\frac{Z_0^2}{Z_0 + Z_n} \tag{2}$$

6

Since $z(t) \ll Z_0$, we can assume $Z_n \gg Z_0$ and therefore

$$z(t) = -\frac{Z_0^2}{Z_n} \qquad (3)$$

Assuming a uniform current distribution in column N, and the conducting material to be of homogeneous and of resistivity $\rho$ and volume $v$, the impedance of the column N is

$$Z_n = \rho \frac{L}{v/L} \qquad (4)$$

And therefore the impedance variation is given as

$$z(t) = -\frac{Z_0^2}{\rho L^2} v \qquad (5)$$

Impedance cardiography shows a pulsatile change in impedance. Initially an assumption was made that the inflow of blood into the lungs is the source of the impedance change. Just before systole, the volume of column N is zero. As the blood volume in the lungs increases during the systole, the impedance decreases and assuming that no blood leaves the lungs during systole. The maximum change in the blood volume $\Delta V$ is the same as the stroke volume and using equation (5), it can be related to maximum change in the impedance $\Delta Z$

$$\Delta Z = (-z)_{\max} \qquad (6)$$

$$\Delta V = \rho \frac{L^2}{Z_0^2} \Delta Z \qquad (7)$$

The equation (7) for the estimation of the stroke volume is known as Kubicek's formula.

7

### 2.4.1 Derivation for Stroke Volume

According to Kubicek's model, change in impedance $z$ is maximum during systole. Therefore,

$$\Delta Z = (-z)_{max}$$

Equation (6) gives the expression for change in blood volume $\Delta V$ in terms of thoracic impedance change $z$.

$$\Delta V = \rho \left( \frac{L^2}{Z_0^2} \right) \Delta Z$$

$\Delta V$ = the maximum volume change in small parallel column

$\rho$ = the resistivity of the material in parallel column

$L$ = the length of the column

$Z_0$ = the impedance of the fixed conduction volume

$\Delta Z$ = the maximum impedance change across the column

The stroke volume is defined as the volume of blood that enters the lungs during systole. The above equation relates the impedance change to the net blood volume change, which reflects the difference between the arterial inflow and venous outflow. To account the blood that leaves the lungs during systole, a forward extrapolation slope procedure is suggested by R.P.Patterson et al. [5]. As shown in Fig 2.5, a straight line is drawn parallel to the steepest part of the early impedance change. This procedure assumes that the pulmonary arterial flow profile is a square wave lasting till the end of the systole and that significant outflow from the lungs does not occur until the later part of the systole. Therefore the early rise in the impedance pulse is only due to arterial inflow into the lungs. The extrapolation of $z$ is obtained using the product of negative peak (minimum) of $dz/dt$ and the ejection time which is determined from the last upward crossing of $dz/dt$ before the large systolic peak to the most downward deflection of $dz/dt$, which corresponds to the end of systole.

Thus $z$ can be calculated as

$$z = \left( -\frac{dz}{dt} \right)_{max} T_{lvet}$$

where $T_{lvet}$ is the ejection time between systole and diastole. Thus, Kubicek's formula is modified and written as the following expression for estimation of the cardiac stroke volume

$$\text{Stroke Volume} = \frac{\rho L^2}{Z_0^2} \left( -\frac{dz}{dt} \right)_{max} T_{lvet}$$

where  $\rho$  =  blood resistivity

        $L$  =  distance between the voltage sensing electrodes

      $Z_0$  =  basal impedance of the subject

$(-dz/dt)_{max}$  =  peak value of the $z$ derivative measured from the base line

    $T_{lvet}$  =  left ventricular ejection time

## 2.5   The impedance cardiogram

A typical impedance cardiogram is shown in Fig 2.5. The upper waveform shows the $-z(t)$ variation. To get the impedance cardiogram, $-z(t)$ is subjected to differentiation. Then there is a negative peak for the $-z(t)$ waveform. The PCG and ECG signals are synchronized with impedance cardiogram. From this waveform, different activities in cardiac cycle can be reveled [6]. 'A' wave corresponds to the atrial systole. It appears approximately 40-100 ms after 'P' wave of the ECG. During the closure of aorta, impedance is slightly higher. 'B' wave shows the instant of aortic valve opening. This is the start of ejection of blood from the ventricle and sychronised with the first heart sound. 'C' wave corresponds to ventricular systole. It is the largest decrease in impedance during systole. Peak 'C' coincides with peak pulse flow time measured on aorta. 'X' and 'Y' correspond to aortic and pulmonary valve closure. 'O' wave shows the largest decrease in impedance during ventricular diastole. It is very close in time to mitral valve opening.

9

Fig 2.6 shows the impedance cardiogram synchronised with cardiac cycle. In this figure, pressure changes in aorta, pulmonary artery and vein are shown. The pressure rise in blood vessels while opening of valves shows large volume of blood into the lungs and peripheral organs. This increased volume of blood gives a time varying impedance change $-z$. The negative sign of $z(t)$ waveform shows a decrease in time varying impedance.

## 2.6 Impedance cardiography technique

The technique involves, sending the current from a constant current source at high frequency (40 kHz–500 kHz) to the thoracic region and measure the voltage variation according to the impedance change $z(t)$. The impedance change $z(t)$ is modulated by high frequency current. Impedance cardiography technique uses a tetra-polar electrode configuration, with a pair of outer electrodes $I_1$ and $I_2$ to inject a constant current and another pair of inner electrodes $V_1$ and $V_2$ to pick up the voltage drop across the thorax region. The threshold of perception for human subjects at high frequencies is in the order of tens of milliamperes [7]. The constant current sent to the thorax is approximately 5 mA. Basic block schematic for impedance cardiograph [8] is shown in Fig 2.7. To extract the signals $z(t)$ and $Z_0$, an instrumentation amplifier, amplitude demodulator and amplifiers are used. The placement of electrodes serves an important role in the impedance measurement.

Table 2.1. Resistivity of biomaterials measured by Baker at 100 kHz [4].

| Tissue | Resistivity ($\Omega$.cm) |
|---|---|
| Blood | 150 |
| Skeletal muscles | 300 |
| Cardiac muscles | 750 |
| Lung | 1275 |
| Fat | 2500 |

# Chapter 3

# Earlier Development

## 3.1 Introduction

This chapter describes the hardware and software development for impedance cardiography done earlier at IIT Bombay. The activity of developing the system has been carried out from 1990 onwards, as a part of student projects by D.V.Nagvenkar [9], H.Lakdawalla [10], S.M.Joshi [11][12], and K.S.Patwardhan [13]. In 1997, Patwardhan developed a hardware based on the technique used by Qu *et al.* [8]. The signals output from the instrument were interfaced to (a) a PC with data acquisition card, (b) a notebook PC with PCMCIA interfaced data acquisition card, (c) a data logger for signal acquisition during testing and download to PC later on. The signal analysis and display was done on the PC. For the use of the system in field activities, the data logger interface is used. This chapter provides a brief description of this system and outlines the need of further development.

## 3.2 Instrument description

Fig 3.1 shows the block diagram of the impedance cardiography system developed by K.S.Patwardhan [8]. A brief explanation of the instrument is given below.

### 3.2.1 Current excitation

The current excitation circuit is used for injecting a high frequency current to the subject's thorax. The block schematic of current excitation circuit is shown in Fig 3.2. To generate a stable high frequency sinusoidal signal, a Wein-bridge oscillator circuit is used. To provide a current source excitation, the oscillator output is given to a voltage-to-current converter circuit. The excitation current is injected to the subject through a pair of suction cup electrodes. For voltage sensing, another pair of suction cup electrodes is used. The signal is then fed to an ICG extraction circuit for signal conditioning.

11

## 3.2.2 ICG extraction

ICG extraction circuit gives $Z_0$, $dz(t)/dt$ and $d(ECG)/dt$ signals. The block schematic of the ICG extraction unit is shown in Fig 3.3. The front end of the instrument is an instrumentation amplifier with a 16 kHz high pass filter at the input. It is used for eliminating the power line interference, ECG and other motion artifacts. To demodulate the signal a full wave precision rectifier followed by a first order lowpass filter with cutoff frequency of 0.72 Hz is used. The filtered signal consists of basal impedance $Z_0$, changing impedance $z(t)$ signal and large amount of respiration components. Since the respiration signal amplitude is much larger than cardiac impedance signals, they are removed using a DC cancellation circuit. This circuit was developed by Joshi and Pandey [12] as a modification of the circuit earlier described by Qu *et al*. This circuit consists of a window comparator, used for comparing the incoming signal with a threshold voltage and eliminates the respiration component. Then impedance signal is amplified and fed to a differentiator having a corner frequency of 50 Hz. The output of differentiator gives the $dz(t)/dt$ signal.

Another instrumentation amplifier amplifies the ECG signal. It is used to provide a fiducial mark for each heart beat. To reduce the effect of large artifacts at low frequency, a first order high pass filter with corner frequency around 1 Hz is used. The signal is differentiated using a differentiator with a corner frequency of 15 Hz to get $d(ECG)/dt$ signal. The current excitation and ICG extraction circuits are assembled in separate PCBs and packed in a box.

## 3.2.3 Thorax Simulator

To calibrate the ICG extraction instrument, a thorax simulator is built. This unit contains one ECG simulator and impedance simulator. ECG simulator is made up of one astable multivibrator followed by four monosatble multivibrator circuits connected in series. The RC time constant of each monoshot is designed proportional to the time intervals of QRS complex in ECG. P and T waves being not important in the simulation of ECG waveform, have not been simulated.

Impedance simulator is sycnhronised with the simulated ECG waveform. The R point of ECG is detected and monoshots are used for its waveform generation. The waveforms from monoshots are integrated to get a triangular waveform, for controlling the impedance variation. The thorax impedance is modeled as a resistance (basal impedance) in parallel with a varying resistor. The variable resistance is realized using a JFET circuit. The electrodes are replaced by its equivalent contact resistance of 220 $\Omega$. The thorax simulator is fabricated in a separate box. The simulator unit has four terminals, two for injecting the sinusoidal current from the current excitation source and two for pick up the amplitude-modulated waveform which are connected to the ICG extraction circuit.

### 3.2.4 Power supply

The power supply required for ICG extraction circuit is a dual supply of ±9 V, 65 mA .It is directly taken from a DC power supply instrument @18V dc. A split circuit using op-amp in the instrument converts 18 V into ±9 V. For thorax simulator circuit, single supply of 9 V from DC power supply instrument is used.

## 3.3  Signal acquisition and processing

The estimation of the cardiac output (CO) requires the knowledge of heart rate (HR) and stroke volume (SV) which are obtained by processing the digitized $d(ECG)/dt$, $Z_0$ and $dz(t)/dt$ signals. In the system developed by Patwardhan, the signal acquisition can be done by one of the three setups,

    a. Signal conditioner is interfaced to a PC through PC bus based data acquisition card PCL-208 (Dynalog Microsystems).

    b. Signal conditioner interfaced to a note book PC through a PCMCIA – bus based data acquisition card,  DAQ700 (National Instruments).

    c. Signal acquisition by a data logger for signal recording and down loading the data to a PC for off-line processing.

A signal acquisition and processing program was developed for the first two setups. The use of the third setup requires a different program for signal acquisition although processing remains the same.

## 3.4 Further developments needed

As a part of the current project, some tests were conducted on actual subjects and waveforms were recorded. The effect of 50 Hz noise pickup was observed in the waveforms. The electrode wires were replaced by coaxial cables, which reduces the power line interference. The circuits were boxed and interconnected. With the above working setup, some experiments were done on a subject. The waveforms were noted using storage oscilloscope and printouts were obtained.

The whole hardware was built on four PCBs. Some of the wiring done in the boxes were re-soldered to ensure connection between the PCBs. It was noted that the components on PCBs are well arranged but still the PCB size can be further reduced. The wiring between PCBs may create open circuit at the time testing or debugging of the circuit. The connectors used for electrode also need some modifications.

It was decided to reassemble all the circuit blocks, thoroughly test all the waveforms and reselect the components for the desired performance and then redesign the PCB in-order to build a portable, reliable system.

The thorax simulator circuit is very elaborate in ECG simulation but it is difficult to use for calibration and needs to be modified.

# Chapter 4

# Hardware description

## 4.1 Introduction

This chapter explains the hardware details. The block schematic of the instrument is same as shown in Fig 3.2 and 3.3 earlier. To excite the impedance under study, a 100 kHz sinusoidal signal with constant current of 3 mA rms is generated. This is applied to the current sending electrodes. During sensing, the changing thoracic impedance results in amplitude modulated voltage waveform. This modulated carrier also has the subject's chest ECG riding over it. Signal conditioner circuit extracts the ECG and the ICG signals of the subject. The final outputs of signal conditioner circuit are $Z_0$, $dz(t)/dt$ and $d(ECG)/dt$ waveform.

Resistor and capacitor values in the op-amp circuits have been reselected to improve the performance. A high contact impedance indicator circuit is designed and implemented for indicating the operating status of V/I converter [14]. The thorax simulator used for the calibration of the signal conditioner unit is modified. In the earlier instrument, the simulator circuit is implemented using several monoshots and one JFET, which increased the complexity of the circuit. This circuit attempts to simulate both the ECG waveform and impedance variation. For calibration purpose, actual wave pattern of ICG and ECG are not necessarily required. Step change input can be used for finding the response of the sensing circuits.

Various parts of the instrument hardware like, current excitation, signal extraction and power supply requirements are described.

## 4.2 Electrodes

### 4.2.1 Tetra-polar electrode configuration

For impedance measurement, basically there are two electrode configurations namely, bipolar (2-electrode) lead configuration and tetra polar (4-electrode) lead

15

configuration [3]. The equivalent resistor network for 4-electrode configuration is shown in Fig 4.1. Four points are selected in a resistance block in such a way that the voltage across the impedance $Z_x$ is to be measured. $E_1 - E_4$ represents four electrodes connected. For measurement, a constant current source is connected across the outer terminals of the resistance block. If $Z_x$ is varying, the variation in voltage across $V_{Zx}$ is proportional to its impedance change. The amplifier (gain=A) for measurement of $V_{Zx}$ should have very high input impedance,

$$Z_{in} >> (Z_x + Z_{V1} + Z_{V2})$$

Then the output voltage is

$$V_0 = A \cdot I \cdot Z_x$$

In this arrangement, $V_0$ is not affected by impedance other than $Z_x$. For thoracic impedance sensing, the current injecting electrodes are placed at outer ends of the thorax under measurement. The voltage sensing electrodes are placed in between the resistor block to detect maximum impedance variation.

Four suction type ECG electrodes are used for measurement of ICG. The electrodes are dipped in electrode gel before connecting to the subject's body to ensure good electrode-skin contact. These electrodes are non-polarizable type, which eliminates the half-cell potential [7]. The suction cup electrode is shown in Fig 4.2. One pair of electrodes is used for sending a sinusoidal current across the impedance under measurement and second pair is used for sensing the voltage across it.

The placement of electrodes for impedance measurement is shown in Fig 4.3. Electrodes are to be placed in such a way that motion artifacts are reduced. One current electrode is placed on the back of the neck behind the cervical vertebra C4 and the other is placed on the vertebra T9. This scheme is proposed by Qu *et al.*[8]. Current electrodes are named as electrodes 1 and 4. Sensing electrodes are used to pickup the voltage developed across the impedance under study, which are named as electrodes 2 and 3. One electrode is placed 4 cm above the clavicle on the front of the neck and the other is placed on sternum at the fourth rib.

## 4.3 Current excitation

### 4.3.1 Oscillator circuit

A Wien-bridge oscillator circuit shown in Fig 4.4 is used for generating 100 kHz, 9 $V_{p.p}$ sinusoidal signal. It is built around op-amp $IC_{12}$. With this oscillator frequency and amplitude, neither the nerves nor heart muscles can be stimulated. The oscillator frequency is given as

$$F = \frac{1}{2.\pi.RC}$$

where $R = R_{57} = R_{58}$ and $C = C_{19} = C_{20}$. With the values as shown in the Fig 4.4, $F = 106$ kHz.

The amplitude of the oscillator is stabilized using the circuit around JFET $T_1$ and zener diode $D_7$. If the negative half cycle of the output voltage exceeds the zener breakdown, excess voltage is filtered in RC network provides $V_{GS}$ bias for JFET. Thus channel resistance of JFET increases, reducing the effective gain of the amplifier circuit and hence its output amplitude. Thus amplitude of the oscillator circuit is stabilized. The output voltage is converted to proportional current by V/I converter.

### 4.3.2 Voltage-to-current converter

A voltage-to-current converter as shown in Fig 4.4 is used to send a constant current to the impedance under measurement. An op-amp $IC_{13}$ circuit is used as the current source where the current flowing through resistor $R_{59}$ at the input is set to be constant. The tissue under measurement is connected in feedback loop of the op-amp where the current flow is constant. The constant current flowing through $R_{59}$ can be obtained as

$$I_s = \frac{V_s}{R_{59}}$$

The output amplitude from Wien-bridge oscillator is 3 $V_{rms}$. Then $I_s = 3$ mA rms. This current is injected to the thoracic region.

17

The voltage variation according to impedance change is directly available from the voltage sensing electrodes $V_1$ and $V_2$. The current electrodes are connected through dc blocking capacitors $C_{23}$ and $C_{24}$, with values selected so that they offer negligible impedance (compared to the basal impedance $Z_0=22$ $\Omega$) at the excitation frequency. In case of loose contact of the electrodes to the skin, $Z_x$ will be very high, and op-amp $IC_{13}$ may be driven to saturation. To avoid this possibility, the resistor $R_{60}$ ($=2.2$ k$\Omega$) has been put in parallel with electrodes. It also helps in reducing the dc errors.

At high frequencies, an alternating current through the body segment results in electromagnetic stray fields that reduce the amount of current actually injected into the tissue under study. This radiation effect can be reduced by a symmetrical configuration current source [15]. A transformer-less balanced current source was designed and tested. Its description is given in Appendix A. However, it has not been implemented as a part of the instrument.

### 4.3.3   Contact impedance indicator

The contact impedance indicator circuit is used to verify the firmness of contact at the skin-electrode interface, and operation status of V/I converter with the rectified (corresponding polarity) average value of the oscillator output [14]. The circuit diagram is shown as a part in Fig.4.4. Two indicator circuits with LED are used for this purpose. Each circuit compares the amplitude level of one half cycle of the sinusoidal waveform. When electrodes are not connected to the subject or simulator, the level in both positive and negative half cycles will become high and both LEDs are turned on. When both LEDs are turned OFF, V/I converter is operating in active region. V/I converter may go into saturation due to increased input bias current, or other dc errors. If either one LED is on, it indicates that corresponding half cycle is in saturation.

## 4.4   ICG extraction circuit

The ICG extraction circuit consists of an instrumentation amplifier for picking up and amplifying the amplitude modulated voltage, demodulator for obtaining the *z(t)*

18

waveforms, low-pass filter for obtaining the basal impedance $Z_0$, DC cancellation circuit for removing respiration artifacts and differentiator for observing $dz(t)/dt$. These circuits are described in following subsections.

### 4.4.1 Instrumentation amplifier for ICG

The voltage electrodes (2 and 3) sense the 100 kHz voltage signal across thorax, which has been modulated by the changing thoracic impedance. The instrumentation amplifier circuit is made using three op-amps $IC_1$, $IC_2$, $IC_3$ as shown in Fig 4.5, and its function is to amplify the sensed difference voltage, and reject the ECG components, low frequency artifacts, and common mode voltages. The input signal is high pass filtered using a passive first order high pass filter ($C1$-$R_1$, $C_2$-$R_2$) circuit having a cutoff frequency at 16 kHz. The differential gain of the amplifier is 20. The expression for gain of a differential amplifier is given by

$$\text{Gain} = \left(1 + \frac{2.R_{f1}}{R_{i1}}\right)\frac{R_{f2}}{R_{i2}}$$

where $R_{f1} = R_4 = R_6$ and $R_{i1} = R_5$

$R_{f2} = R_8 = R_9 + R_{10}$ and $R_{i2} = R_3 = R_7$

With the values shown in Fig 4.5, overall gain obtained is 17.34. In order to obtain a high CMRR, ±1% precision resistors are used. Resistor $R_{10}$ is a 10-turn cermet potentiometer in the second stage adjusted for highest CMRR at the excitation frequency. The op-amps used are CA 3100 having $f_T = 38$ MHz [16]. Each op-amp is compensated with a single 22pF capacitor. The output signal obtained from the instrumentation amplifier is proportional to the modulated cardiac impedance variation. For demodulation, this signal is fed to an amplitude demodulator.

### 4.4.2 Demodulator circuit

The demodulator circuit is a rectifier detector consisting of full wave precision rectifier followed by a first order low pass filter. The rectified signal is low pass filtered

to remove the 100 kHz carrier signal. A synchronous detector may have resulted in better signal-to-noise ratio. However in this case, the modulation index is very low (<<0.01) and we do not expect interference at about the carrier frequency [17].

The circuit diagram of the demodulator is shown as a part of Fig.4.5. It consists of a full wave precision rectifier using op-amps $IC_4$, $IC_5$ incorporated with a low pass filter. This is used because, a high pass filter at 16 kHz is used at front end of the ICG extraction circuit. This filter eliminates 50 Hz noise pickups, ECG signal and passes ICG signals. The variation in the impedance is purely resistive at 100 kHz and there is no phase variation in the detected signal. The op-amps, CA 3100 and diodes, 1N 4148 used for rectification are fast enough at 100 kHz. The low pass filter has upper 3-dB cutoff frequency at 30 Hz and provides smoothing of the rectified signal. This is achieved by $R_{17}$-$C_9$. This also eliminates 50 Hz noise interference. The output of the demodulator represents the thoracic impedance $Z(t)$. The waveform $Z(t)$ consists of the basal impedance $Z_0$ , changing impedance $z(t)$ and possibly some respiration artifacts. To extract $Z_0$ from $Z(t)$, it is severely low pass filtered. This low pass filter has a 3-dB cut-off frequency of 0.7 Hz and attenuates variations in $z(t)$ signal that arises due to respiration and body movements. This is achieved by $R_{20}$-$C_{10}$. The respiration component is to be removed from the $Z(t)$ signal. Hence a DC cancellation circuit is used. The output of DC cancellation circuit gives $z(t)$.

### 4.4.3 DC cancellation circuit

To extract the changing thoracic impedance component $z(t)$ from respiratory artifacts, a DC cancellation circuit is used. The circuit diagram is shown in Fig 4.6. It consists of an amplifier, window comparator and integrator. Two quad op-amp chips are used for its implementation. The signal input is amplified and inverted. A window comparator is designed using two op-amps, which are operating with reference to a threshold level input controlled by a potentiometer $R_{28}$. The window comparator output is given to an integrator circuit. The output of the integrator is fed back to the input, which subtracts from the incoming signal.

20

The respiration component is a slow varying signal with amplitude much greater than $z(t)$ component. The value of threshold voltage $V_{th}$ is made greater than the normal strength of $z(t)$ component but less than that of the respiration component. When the input amplitude exceeds the threshold level due to respiration components, one of the comparator output makes corresponding diode conducting. This dc signal is integrated and an opposing voltage corresponding to respiration component is fed back to the input of the DC cancellation circuit. Now the fast changing low amplitude $z(t)$ component escapes unaffected and rest of the signal gets cancelled out. The RC time constant of integrator circuit is set to 200 ms, fast enough to remove the respiration component. This is achieved by $R_{32}$-$C_{11}$. The five op-amps used for DC cancellation are from two LM 324 ($IC_6$, $IC_7$) chips. The remaining three op-amps from these chips are used in the circuits for $Z_0$ output, amplifier for $z(t)$ and differentiating $dz(t)/dt$ signal. These op-amps reduce complexity in PCB design of the circuit.

### 4.4.4 Differentiator circuit

The z amplifier and differentiator circuit is given in Fig 4.7. The output of the DC cancellation circuit gives $z(t)$ waveform. A non-inverting amplifier further amplifies it. The amplified signal is differentiated by an op-amp circuit ($IC_7$) to get $dz(t)/dt$ signal. The nominal value of the differentiator corner frequency is 50 Hz. The cut-off frequency is given as

$$F = \frac{1}{2.\pi.R.C}$$

Using $R_{38}$ and $C_{13}$ the cut-off frequency is 53 Hz. The maximum frequency content of the $z(t)$ signal comes around 30 Hz.

### 4.4.5 ECG extraction circuit

The ECG extraction circuit is shown in Fig 4.8. The ECG of the subject is also obtained from the same voltage sensing electrodes. The ECG signal is given to another instrumentation amplifier using op-amps $IC_8$, $IC_9$, $IC_{10}$ having a gain of 15, which

21

amplifies only the low frequency components. It has a low pass filter having a 3-dB cut off frequency of 40 Hz and removes all 100 kHz carrier component from the ECG signal. This is achieved by $R_{46}$-$C_{13}$, $R_{47}$-$C_{14}$. The output of the instrumentation amplifier is high pass filtered, using a passive differentiator having a cutoff frequency around 0.2 Hz. This is achieved by a passive differentiator circuit using $R_{51}$-$C_{16}$. Thus the base line drift is attenuated and gives *d(ECG)/dt*. A non-inverting amplifier further amplifies this ECG. It has an active differentiator ($IC_{11}$) with a 3-dB cutoff at 12 Hz to remove 50 Hz noise. This is achieved by $R_{49}$, $C_{16}$. Here *d(ECG)/dt* signal is used as a reference mark for *dz(t)/dt* signal.

### 4.4.6  Power supply

The ICG instrument is using a ± 12 V, dual dc power supply. This can be given from a DC power supply instrument or using batteries. The total current consumption is approximately 70 mA. All integrated circuits are properly de-coupled using $0.1\mu F$, 25 V ceramic disc capacitors. All high frequency chips (CA 3100) are externally compensated using 22 pF ceramic capacitors.

## 4.5  Thorax simulator

The impedance cardiography technique for monitoring stroke volume and cardiac output requires extraction of the subject's ECG and ICG. The ICG is differentiated to get *dz(t)/dt*. It will be very useful to have a hardware simulator to verify the proper operation of ECG and ICG circuits. The block schematic of a thorax simulator is shown in Fig 4.9. The thorax simulator simulates

1.  The thorax impedance consisting of a fixed impedance $Z_0$ and varying impedance *z(t)*.
2.  ECG signal with common mode and difference mode components.
3.  Common mode interference waveform.
4.  Tissue-electrode contact resistance.

This can be used for the calibration and testing of the impedance cardiograph circuit.

22

A step change in the impedance can be used for finding the sensitivity and response time (or bandwidth) of the impedance sensing circuit. The frequency and level of impedance change should be variable.

The thoracic impedance can be as a resistive network as shown in Fig 4.10. $R_0$ is the basal impedance (shown as two resistors of value $R_0/2$ each). $R_s$ in series with a switch causes a variation

$$\Delta R = (R_s \parallel R_0) - R_0$$

The switch is controlled by pulses, simulating the pumping of blood from the ventricles. Assuming that all the impedance variation takes place only in the region between the voltage electrodes, the fixed resistors $R_{C1}$ and $R_{C2}$ represent the tissue resistance in the path of the excitation current. Resistors $R_{e1}$ and $R_{e4}$ represent the tissue-electrode contact resistance for current excitation. Similarly, $R_{e2}$ and $R_{e3}$ represent tissue-electrode contact resistance for the two voltage sensing electrodes. The voltage source '$e_d$' represents the differential ECG signal. The voltage source '$e_c$' represents all the common mode pickups. In the actual implementation, the effects of impedance variation, ECG signal and common mode pickup can be simulated independently. However, since the ECG signal and the impedance variation are pulsatile, only one simulation can be activated at a time, for studying their effects separately.

The implementation is schematically shown in Fig 4.11. The switchable resistance $R_s$ has been split into two resistors $R_a$ and $R_b$ ($R_a = R_b = R_s/2$) symmetrically placed on two sides of the switch. The differential and common mode ECG signals are introduced with the two sources '$e_1$' and '$e_2$' and the voltage attenuator is formed by $R_{x1}, R_{y1}$ and $R_{x2}, R_{y2}$.

The relationship between circuit parameters as in Fig 4.10 with their reference in Fig 4.11 is given below.

$$R_{c1} + R_{e1} = R_1 , \quad R_{e2} = R_2 , \quad R_{e3} = R_3 \quad \text{and} \quad R_{c2} + R_{e4} = R_4$$

For impedance variation, an analog switch is used, controlled on/off by its control input. Quad CMOS analog switch CD 4066, [18] has been used with all the four

switches connected in parallel to reduce "on" resistance. The resistance offered by each switch at $V_{DD}$ =10 V is $R_{s(on)}$ =120 Ω. The relationship between the values in Fig 4.11 and Fig 4.12 are as following.

$$R_{x1} = R_{73} + R_{74}, \quad R_{x2} = R_{79} + R_{80} \quad \text{and} \quad R_{y1} = R_{72}, \quad R_{y2} = R_{81}$$

$$R_Z = R_{77}, \quad R_a = R_{75}, \quad R_b = R_{78}, \quad R_1 = R_{71}, \quad R_2 = R_{76}, R_3 = R_{82}, \quad R_4 = R_{83}$$

The connection details of the chip as used in the impedance simulator is shown in Fig 4.12. The equivalent thorax resistance $R_{eq}$ calculation is shown below. When control voltage turn on the analog switch, the equivalent resistance is denoted by $R_{eq(on)}$. Then,

$$R_{eq(on)} = R_Z \| ( R_a + R_b + R_{switch} ) \| ( R_{x1} \| R_{y1} + R_{y2} \| R_{y2})$$

We select $R_{x1} >> R_{y1}$ and $R_{x2} >> R_{x1}$; and therefore,

$$R_{eq(on)} = R_Z \| ( R_a + R_b + R_{s(on)} ) \| (R_{y1} + R_{y2})$$

Also $R_{s(on)} << (R_a + R_b )$. Taking $R_Z = 22$ Ω , $R_a = R_b = 820$ Ω and $R_{y1} = R_{y2} = 100$ Ω

We get, $R_{eq(on)} = 19.64$ Ω

With the analog switch turned off, the equivalent resistance is denoted as $R_{eq(off)}$

$$R_{eq(off)} = R_Z \| (R_{y1} + R_{y2}) \| (R_a + R_b + R_{s(off)})$$

$$R_{s(off)} >> R_Z$$

Therefore $R_{eq(off)} = 19.81$ Ω. This resistance is taken as the basal impedance of the thoracic impedance simulator.

Therefore, $\Delta R = R_{eq(off)} - R_{eq(on)} = 0.18$ Ω.

To realize the above $\Delta R$, $R_a$ and $R_b$ are connected in series with the chip. The equivalent contact resistance of electrodes is selected as 220 Ω resistors. To simulate the ECG

signals, appropriate voltage signals are applied across the impedance simulator with proper attenuation in the order of millivolts. For testing as well as calibration, resistors $R_a$ and $R_b$ are changed and corresponding variations in the $z$ are detected.

The circuit diagram for ECG waveform and control signal generator for impedance simulator is shown in Fig 4.13. An astable multivibrator is used to generate the voltage waveforms for the impedance simulator. The time period is adjustable by using potentiometer $R_{84}$. With this circuit both impedance and ECG waveforms simulated one at a time. An SPDT switch is provided for selecting either ECG or impedance signal. The voltages '$e_1$' and '$e_2$' are generated from astable multivibrator output and a non-inverting amplifier connected to it. When simulator is used for ECG calibration, impedance simulator is turned off using LM 311 to provide $V_{ILC} = 0 V$. The op-amps in the circuit are powered from a split power supply, $\pm 4.5$ V derived from a 9 V battery. The split supply is made using LM 741 as shown in Fig 4.14.

## 4.6 Power Supply requirements

ICG instrument and thorax simulator circuits use separate power supplies. ICG instrument it is driven from $\pm$ 9 V to $\pm$ 15 V dual supply. It can be obtained from a single battery by using a DC/DC converter. DC/DC converter, ZUW 3 1212 [19] is used in the instrument. It is thoroughly tested under different load conditions and performance was found to be satisfactory. It delivers $\pm 12$ V, 110 mA from a single supply source varying from 9 V to 18 V dc. The circuit diagram is shown in Fig 4.15. Thoracic impedance simulator circuit uses a 9 V battery, which converts into a split power using an op-amp circuit.

25

# Chapter 5

# Circuit assembly and testing

## 5.1 Circuit assembly

The ICG instrument and the thorax simulator have been built as two independent instruments. Both instruments are battery operated. This helps to reduce the interference of common mode signals as well as electromagnetic pickups and takes care of electrical safety considerations. The ICG instrument is powered by ±12 V dual supply, obtained by using a 9–18 V dc source and DC/DC converter. The thorax simulator circuit is operating from a single 9 V battery with an internal split power supply circuit.

The impedance cardiograph has been built on a single double-sided (with PTH) PCB of size 15 cm × 15 cm. It consists of excitation current source, ICG extraction, ECG detection and contact impedance indicator circuits. The PCB layout has been designed with special consideration for reducing the power supply noise by providing tight coupling between the supply and ground conductors and using decoupling capacitances. The ground is stabilized by providing a large ground plane. For reducing the noise pick-up, the signal lines are coupled with ground track/plane. The PCB has been assembled in a box, with all the switches, controls and indicators at the front side and connectors at the backside. The box has been designed, fabricated and assembled in such a way that the PCB and controls and accessories are fixed on the bottom portion of the box, for easy access to all the circuit parts during testing, once the top cover is removed. All controls, switches and indicators are labeled.

The electrodes are connected with shielded cables and RCA phono connectors. This provides a good shielding for electrode wires and interference problems can be reduced. For each electrode wire, the shield is connected to instrument's 'internal common' terminal at the instrument end and left open at the electrode end.

The thoracic impedance simulator is built on a single sided PCB of size 10 cm × 10 cm with appropriate considerations in the PCB design. This has been boxed separately from the ICG instrument. In front panel of the instrument, impedance/ECG selector switch, time period control for simulating waveforms, common mode/difference mode ECG waveform selector switch, ECG amplitude control and power on/off with LED indicator are given. It has four electrode connectors on the back panel. Along with these connectors, external pick-up and right-leg drive connectors are also given. To get the change in impedance $\Delta R$, two jumper connectors are mounted on the PCB. The top cover of the instrument has to be opened for selecting the desired $\Delta R$ change.

Instrument specifications for ICG extraction unit and thorax simulator are given in Appendix B and C respectively. The list of components is given in Appendix D. The enclosure layouts of both instruments are given in Appendix E and F. The circuit schematics of ICG instrument and thoracic impedance simulator are given in Appendix G. PCB layouts of ICG instrument and simulator are given in Appendix H.

## 5.2   Power supply circuit

The ICG extraction circuit needs ±12 V supply. The current drawn from the two supplies have been measured as $I_{c+}$ = 85 mA, $I_{c-}$ = 90 mA. The ICG extraction unit is working from a 12V battery, converted into a dual supply using a DC/DC converter. The DC/DC converter used has following specifications:

| | | |
|---|---|---|
| DC input voltage | : | 9-18 V |
| Input current | : | 350 mA |
| Output voltage | : | ±12 V |
| Output current | : | 130 mA |
| Output ripple | : | 50 mV$_{p.p}$ at 12 V dc input |

The DC/DC converter is thoroughly tested for the output regulation and ripple, and shows satisfactory operation. There is a provision for placing the DC/DC converter module on the PCB having ICG circuit. However, it has been assembled as a separate

27

module for various applications. The current drawn from the DC power supply source is found to be 350 mA.

The thoracic impedance simulator instrument is working from a single 9 V battery, converted into a dual supply of ±4.5 V using an op-amp $IC_{19}$ split circuit. The split circuit is assembled in the PCB having impedance simulator circuit. The current drawn from the battery was measured to be 8.5 mA.

## 5.3 Testing of thoracic impedance simulator

The thoracic impedance simulator can be used for obtaining either the ECG waveform or the impedance variation. The simulation of ECG waveform and impedance variation is selected by an SPDT switch and the signal is generated by a square wave from an astable multivibrator. The time period of the square wave is adjustable over 0.2 – 2.4 s by using potentiometer $R_{84}$ on the instrument front panel. The ECG simulator has two potentiometers $R_{73}$ and $R_{79}$ for adjusting the levels of '$e_1$' and '$e_2$'in order to control common mode as well as differential mode ECG signals. An SPDT switch is provided to simulate differential mode and common mode ECG signals separately. The ECG waveform appears at the electrode terminals of thoracic impedance simulator needs to be amplified for observations in CRO. The measured common mode ECG variation is 5 – 20 mV and difference mode variation in 5 – 50 mV.

The impedance change is simulated by a change in resistance $\Delta R$, which can be measured using a precision ohmmeter by sending a dc current through the electrode terminals. The resistance variations are tested for different combinations of $R_a$ and $R_b$ shown in Fig 4.12. Table 2 shows the measured $\Delta R$ using ohmmeter for various values of $R_a$ and $R_b$. When a constant current at 100 kHz is applied to the current electrode terminals and if $R_a$ and $R_b$ are selected a low value (approx.150 $\Omega$) amplitude modulated variations are directly observed at the voltage electrode terminals.

## 5.4 Testing of circuit blocks in ICG instrument

The different blocks of impedance cardiograph instrument were individually tested and the results are presented in following subsections.

### 5.4.1 Current injection and contact impedance indicator circuit

The oscillator frequency is 100 kHz. The amplitude of the signal is adjusted by the potentiometer $R_{56}$ (10 k$\Omega$) to get 8.8 $V_{p.p}$ and there is no dc offset.

The V/I converter circuit is tested by changing the feedback resistor $R_{60}$, connected across the current injecting electrodes. $R_{60}$ is selected as 2.2 k$\Omega$ giving 6.84 $V_{p.p}$ across the electrodes, ensured the op-amp is in active region during measurements. During testing, $R_{60}$ is varied up to 5.6 k$\Omega$ giving 18 $V_{p.p}$ and found as the maximum limit for operating the op-amp in active region.

The input voltages for contact impedance indicator circuit are giving from oscillator and V/I converter outputs as shown in Fig 4.4. The LEDs are turned on when electrodes are open and turned off when they are connected after applying electrode gel on skin as well as electrode surface. The LEDs are turned on for square pulses as comparators $IC_{14}$ and $IC_{15}$ are operating according to the input signals from oscillator and V/I converter. The duty cycle of the pulses vary according to the operating status of the V/I converter. When electrodes are open or V/I converter is saturated, duty cycle of square pulses is large, LED brightness increases. When electrodes are properly connected, LED is turned off. When both LEDs are turned off simultaneously, it indicates that both half cycles of V/I converter have same amplitude. When electrode gel is not applied on both electrode surfaces, LEDs are partially on indicating the higher ac resistance at the tissue electrode contact.

### 5.4.2 ICG extraction circuit

ICG extraction circuit consists of instrumentation amplifier, demodulator with lowpass filter, DC cancellation circuit, $z$ signal amplifier and differentiator. All resistors are ¼ W, ±1% tolerance for setting minimum gain in common mode operation. The potentiometer $R_{10}$ (10 k$\Omega$) is cermet type for fine adjustments. The circuit diagram is shown in Fig 4.5. For testing of common mode gain, 8 $V_{p.p}$, 100 kHz sinusoidal signal is

29

given from a function generator. For testing difference mode gain, 500 mV$_{p.p}$ at 100 kHz is applied. The results are given below.

The output measured in common mode is 120 mV$_{p.p}$.

The difference mode gain obtained is 16.72.

CMRR measured is 1066, i.e. 60 dB

To demodulate 100 kHz carrier modulated by impedance variation, a full wave precision rectifier followed by a lowpass filter is used. For testing the response of the rectifier circuit, a difference signal of 1V$_{p.p}$ at 100 kHz is applied to the instrumentation amplifier. The output waveform of the op-amp where the diodes 1N 4148 are connected is noted. The half wave rectified waveform having same shape as input is observed. This indicates switching diodes are fast enough to respond at the operating frequency of 100 kHz.

The low pass filter circuit of amplitude demodulator is tested by observing the dc voltage at the output. The circuit gives a linear variation for varying input voltage. The plot is shown in Fig 5.1. The plot shows a linear variation of output dc amplitude for varying sinewave input amplitude at 100 kHz.

DC cancellation circuit is tested by giving a sine wave of 120 mV$_{p.p}$ superimposed over a slow varying squarewave amplitude, 2 V$_{p.p}$. The output observed from the differentiator circuit shows a cosine wave having amplitude of 10 V$_{p.p}$ after eliminating the slow varying square wave. This shows the DC cancellation circuit is not bypassing the slow varying square wave and sine wave coming out of the circuit is properly differentiated. The circuit diagram is shown in Fig 4.6. Since the amplitude of the sine wave is very small, it is amplified by the $z(t)$ amplifier and differentiated using $dz(t)/dt$ circuit, shown in Fig 4.7. The response time observed is 120 ms. Waveforms recorded at input and output are shown in Fig 5.2 (a) and (b).

The differentiator circuit output gives $dz(t)/dt$ signal. Its corner frequency is set to 50 Hz. The frequency response is plotted and shown in Fig 5.3. To test the circuit an input voltage of 100 mV is given to the $z(t)$ amplifier. The output is observed at pin 14 of IC$_7$ in Fig 4.7.

30

## 5.5 Testing of ICG instrument with thoracic impedance simulator

To find the performance of ICG instrument, the thoracic impedance simulator was connected through four independent shielded cables to the ICG instrument. The measured value $R_o$ = 19.81 $\Omega$ and $\Delta R$ = 0.232 $\Omega$ are obtained by selecting $R_a$= $R_b$ = 820 $\Omega$ with jumper connectors inside the instrument. The injection current from the ICG instrument was 100 kHz sinusoidal signal, 3 mA rms. The time control (H.R.) potentiometer $R_{84}$ of simulator was adjusted to have 1 Hz square wave. The simulator was set in 'ICG' mode for injecting ICG signals into the ICG instrument. While the simulator is in ICG mode, the output of the ICG amplifier were found to be zero. The output at various points in the ICG extraction section of the instrument were observed and are given below.

$V_9$   = 2.42 $V_{p.p}$   Output of ICG instrumentation amplifier

$V_{10}$   = 74 m$V_{p.p}$ square wave superimposed on 6.8 V dc $[Z(t)]$

$V_{11}$   = 7.4 V dc $[Z_0]$

$V_{12}$   = 584 m$V_{p.p}$ squarewave superimposed on $-70$ mV dc

$V_{13}$   = 2.08 $V_{p.p}$ squarewave superimposed on $-500$ mV dc $[z(t)]$

The ac part of $V_{13}$ could be vary from 2.08 V to 4.08 V by adjusting the gain potenetiometer ($R_{35}$). Fig 5.4(a) shows a simulated waveform corresponds to $z(t)$ = 0.232 $\Omega$ and (b) shows its $dz(t)/dt$ waveform. Fig 5.5 shows measured (p.p) output voltage $Z_0$ for different values of $R_0$. Fig 5.6 shows the variation of measured output voltage for of z(t) different values of $\Delta R$.

## 5.6 Recording of waveforms from subject

Some waveforms are recorded from subjects using the ICG instrument. The placement of electrodes is very important to get proper $dz(t)/dt$ waveforms. Electrode gel should be applied to wet both electrode and skin surface. ECG waveforms are available as its differentiated signal ($V_{16}$). The amplitude level of $dz(t)/dt$ in resting condition is 700 m$V_{p.p}$. The $d(ECG)/dt$ amplitude measured is 6 $V_{p.p}$. The recorded ECG waveform is shown in Fig 5.8. Fig 5.9(a) and (b) show recorded waveform of ICG and

31

*d(ECG)/dt* of a subject (ASH) respectively. Fig 5.10 (a) and (b) shows a typical impedance cardiogram and *d(ECG)/dt* recorded from a subject simultaneously. The sample calculation of stroke volume and cardiac output an impedance cardiogram is shown below.

$$\text{Stroke Volume} = \frac{\rho L^2}{Z_0^2} \left( \frac{dz}{dt} \right)_{max} T_{lvet}$$

| | | |
|---|---|---|
| $\rho$ | = | 145 $\Omega$.cm |
| $L$ | = | 16 cm |
| $Z_0$ | = | 20 $\Omega$ |
| $dz/dt_{(max)}$ | = | 7.62 $\Omega$/s |
| $T_{lvet}$ | = | 52 ms |
| Stroke volume = | | 36 ml |
| Heart rate = | | 87 beats/min. |
| Cardiac output = | | 3.13 Liters. |

It is to be noted that there are cycle to cycle variations in stroke volume. Normally, the calculations are done after ensemble averaging of the ICG waveform for large number of cycles. Further the calculations are done using an assumed value of blood resistivity.

Table 5.1 Resistance measurement using ohm-meter in thoracic impedance simulator
(All measurements are in $\Omega$)

| $R_a=R_b(\Omega)$ | Calculated | | | Measured | | |
|---|---|---|---|---|---|---|
| | $R_{off}$ | $R_{on}$ | $\Delta R$ | $R_{off}$ | $R_{on}$ | $\Delta R$ |
| 470 | 19.81 | 19.42 | 0.39 | 20.28 | 19.93 | 0.35 |
| 820 | 19.81 | 19.64 | 0.18 | 20.28 | 20.08 | 0.20 |
| 1200 | 19.81 | 19.66 | 0.15 | 20.28 | 20.11 | 0.17 |

32

# Chapter 6

# SUMMARY AND CONCLUSIONS

## 6.1 Summary of work done

The impedance cardiography is a non-invasive technique that may be used for estimation of cardiac output and for diagnosis of cardiac disorders. In this technique, impedance variation in the thorax according to the changes in blood volume is detected and the measurements are done. The stroke volume and cardiac output can be estimated from impedance cardiogram.

The impedance cardiograph instrument has constant current excitation unit and ICG detector unit. The impedance variations are modulated by sending a high frequency constant current into thorax region. The ICG extraction unit amplifies, demodulates and filters the impedance signal. The instrument output gives differentiated impedance $z(t)$ variation, fixed basal impedance $Z_0$, and differentiated ECG signal. For calibrating the instrument, a thorax simulator instrument is also implemented. It simulates the impedance variation as well as the ECG variation. The instrument is made portable using a battery powered source.

The work involves the redesign, testing and building of ICG extraction unit, designing and building a new thoracic impedance simulator incorporating a contact impedance indicator. The ICG instrument is fabricated in a single PCB to make it compact. The instrument is boxed and battery powered. The contact impedance indicator associated with ICG extraction unit shows the operating status of the current excitation circuit in the instrument. A new thoracic impedance simulator is designed, tested, assembled and boxed separately for the calibration of ICG extraction and ECG extraction circuits. It provides the facility for injecting an external noise pick-up and right leg drive access and is powered from a single 9 V battery.

## 6.2 Suggestions for future work

The instrument developed has to be interfaced with the signal acquisition and analyzer setup and recording are to be made over large intervals. The analysis of the waveform may show further improvement in hardware. The system can be rebuilt for providing the option of varying the excitation frequency.

Balance current source can be employed for reducing the effect of stray magnetic fields, and improvement obtained can be studied.

The instrument can be used for recording waveforms from patients with various disorders in-order to carry out investigation into developing the signal-processing algorithm, for obtaining diagnostic information and estimation of cardiac output.
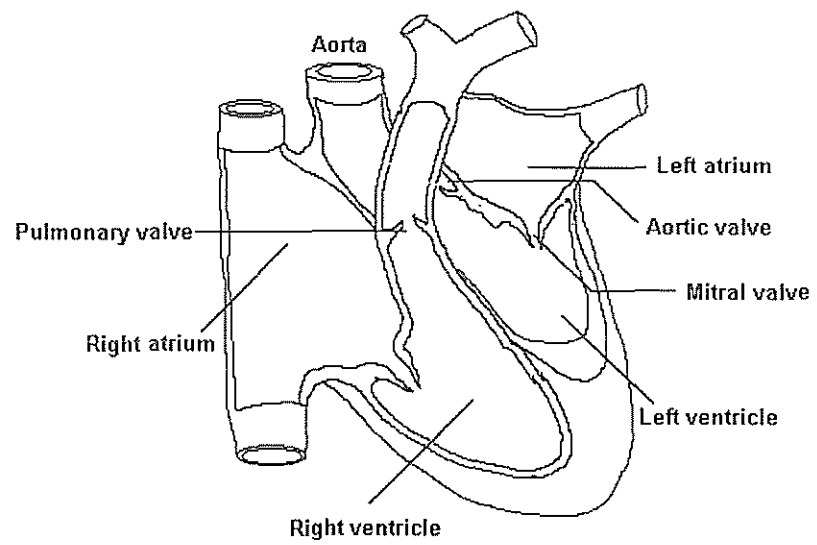
Fig 2.1  Structure of human heart (adapted from [1])
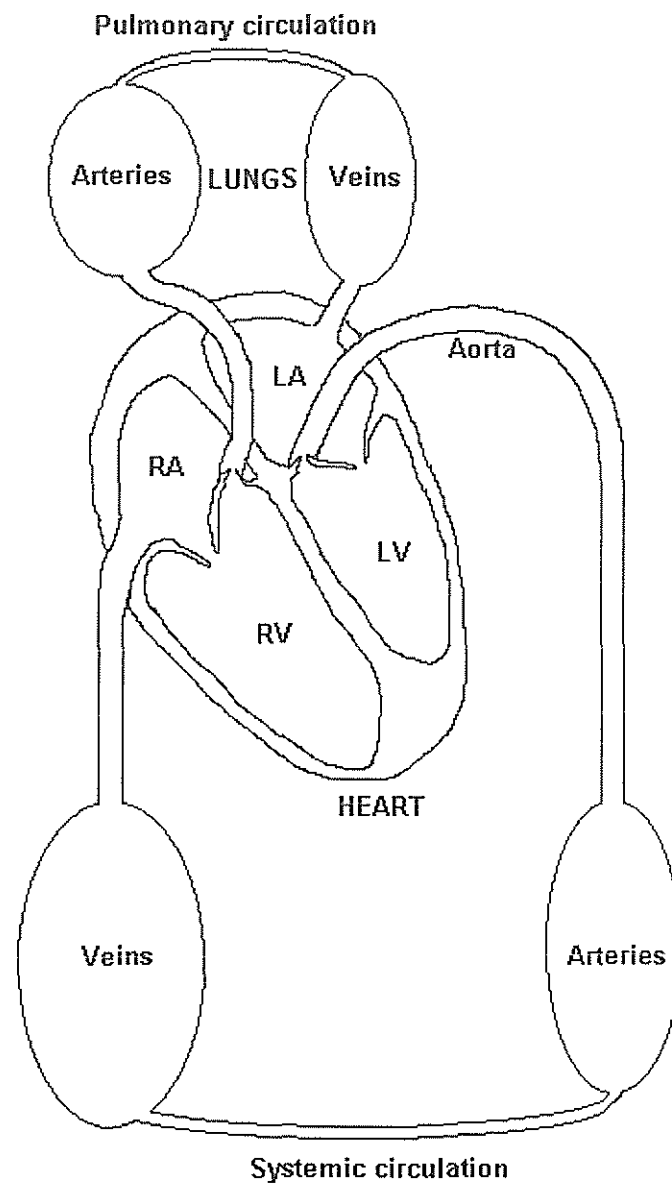
**Fig 2.2 The basic circulatory system** (adapted from [1])
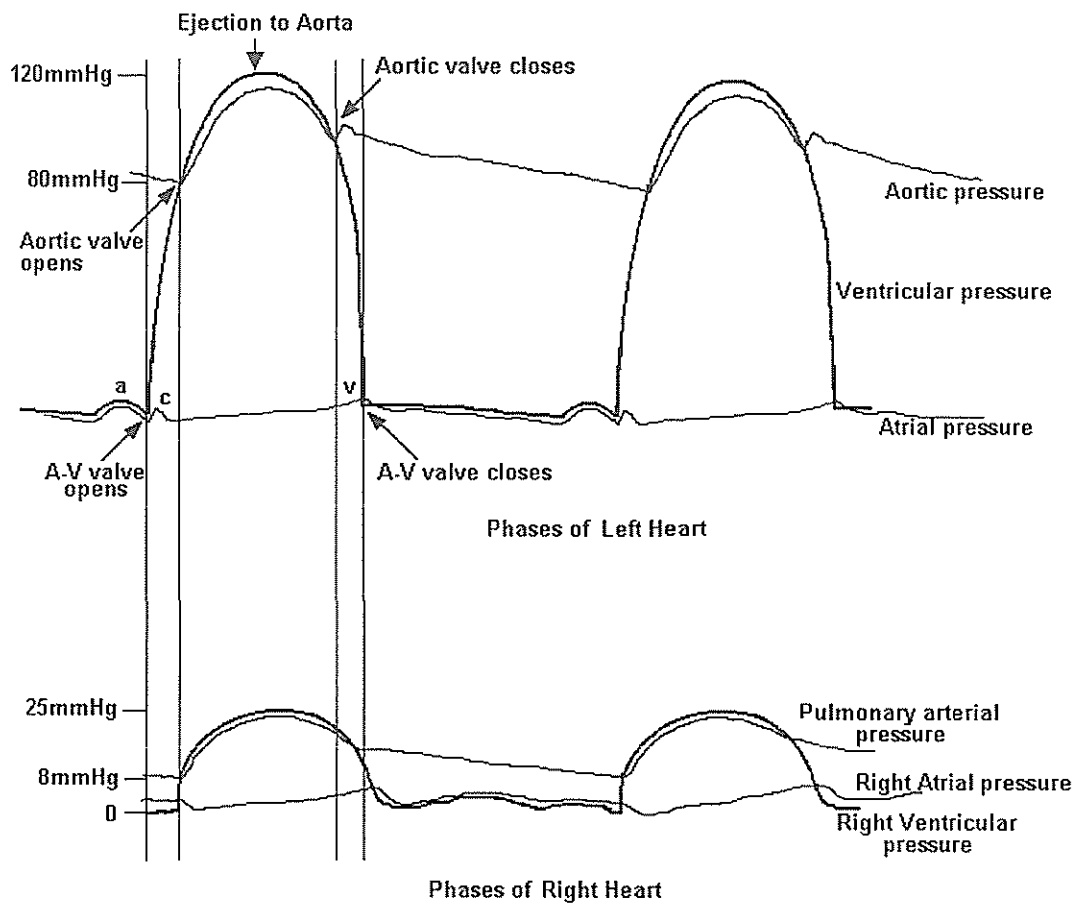
Fig 2.3 The events in a cardiac cycle (adapted from [1], [2])
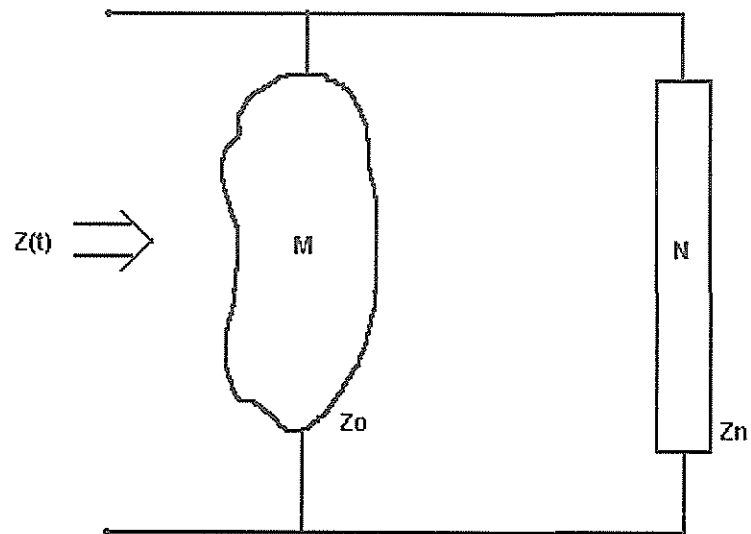
Fig 2.4  Parallel column model ( adapted from [5])
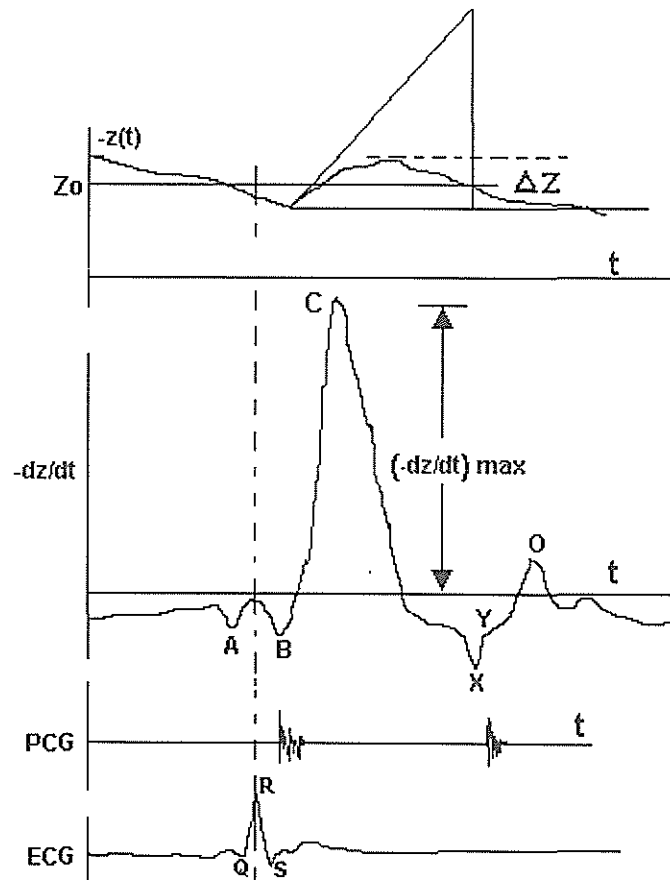


Fig 2.5  Typical impedance cardiogram ( adapted from [5])
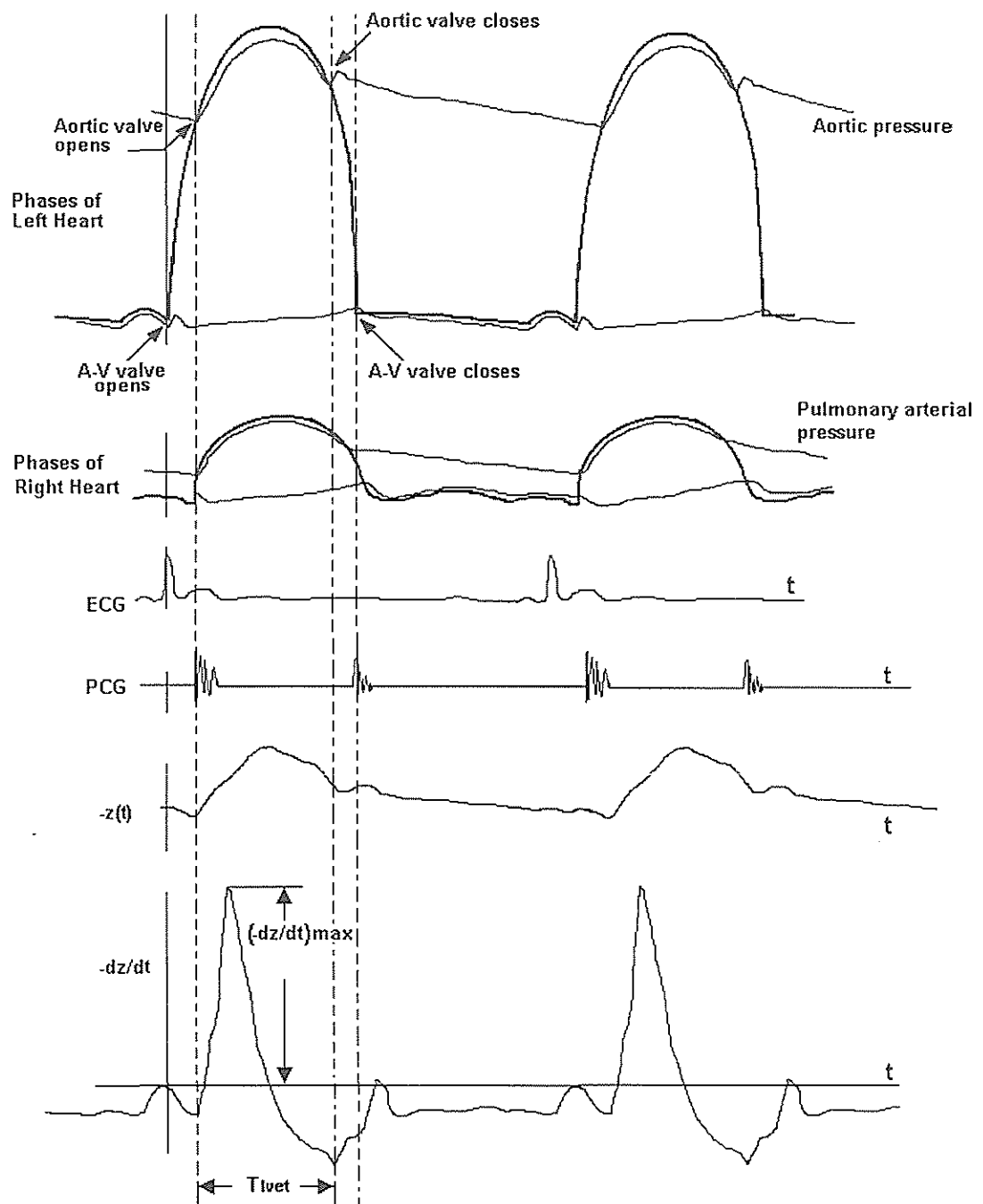
Fig 2.6 Synchronised cardiac cycle and impedance cardiogram.
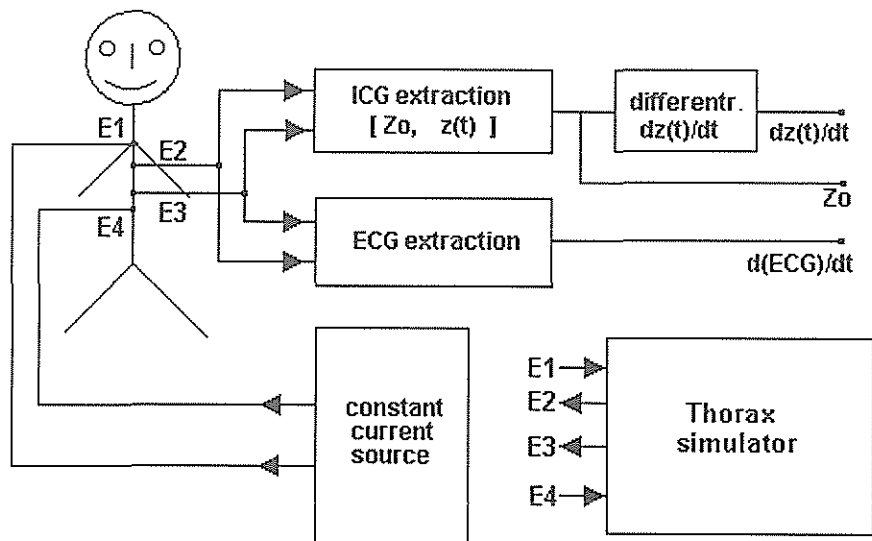
Fig. 2.7 Block diagram of ICG instrumentation
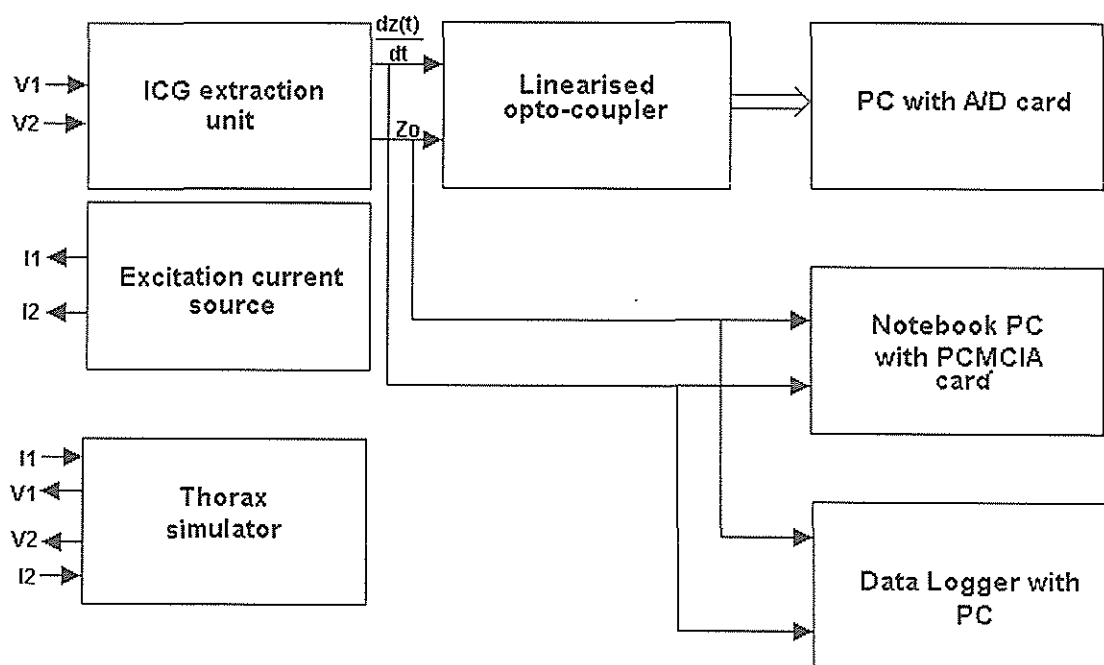


Fig 3.1 Basic block schematic of ICG system ( source - [13] )

40
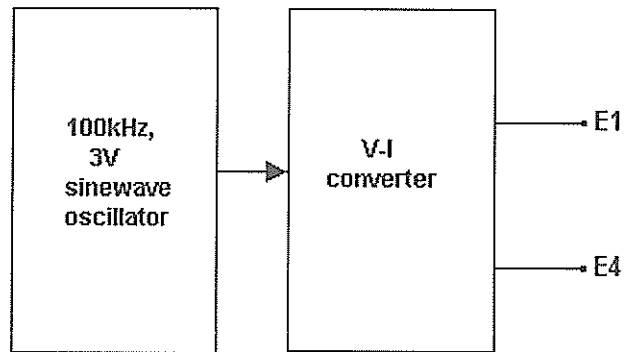
Fig. 3.2 Excitation circuit -block schematic
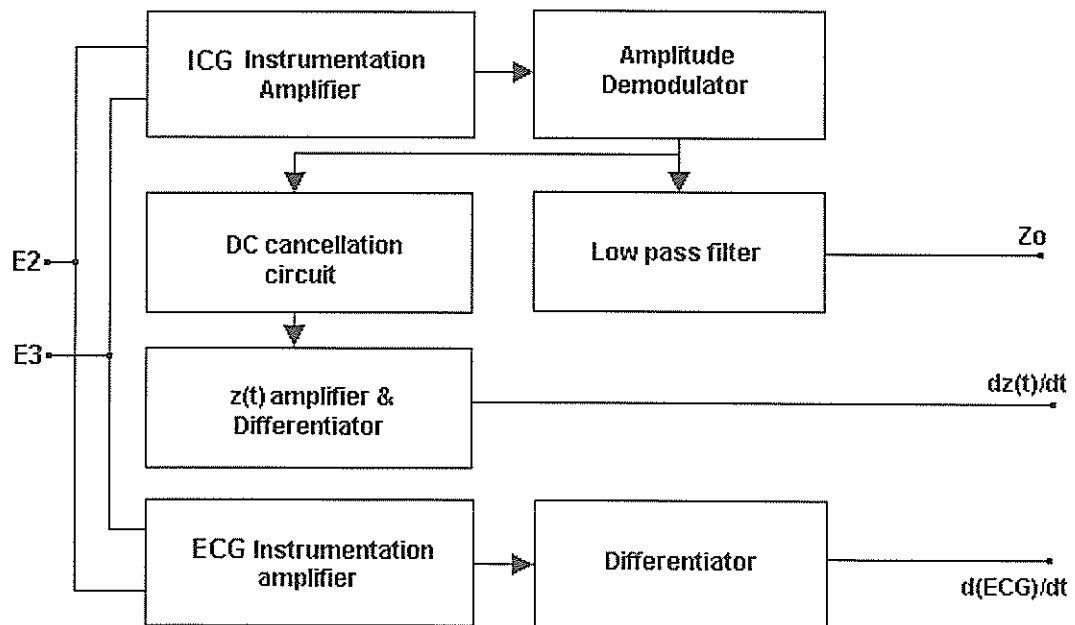


Fig. 3.3 ICG extraction block schematic
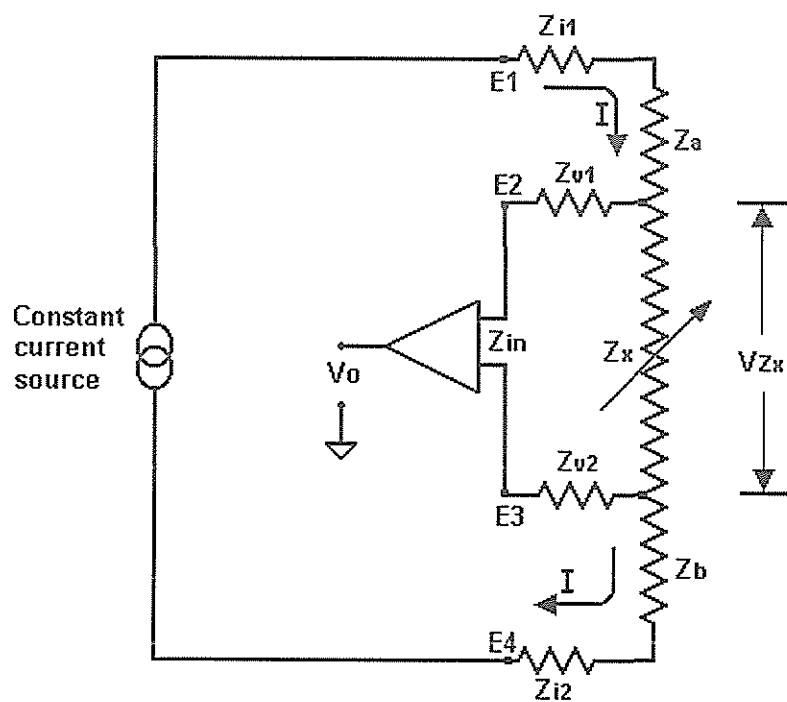
Fig 4.1 Tetra-polar electrode configuration
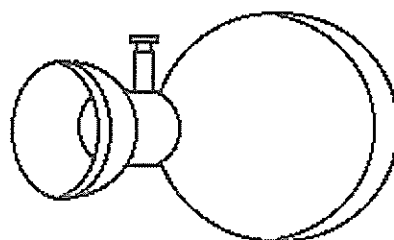


Fig. 4.2 Suction Cup electrode

Anterior       Posterior
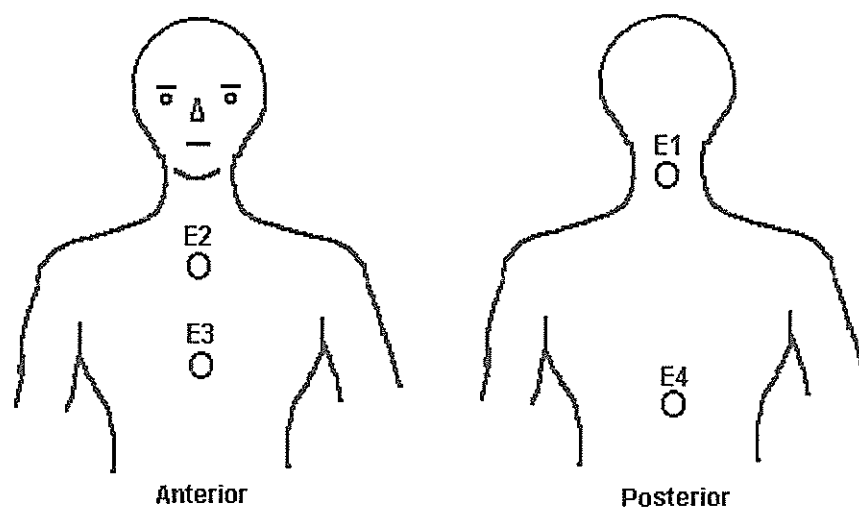
Fig 4.3 Electrode placement scheme ( adapted from [8] )
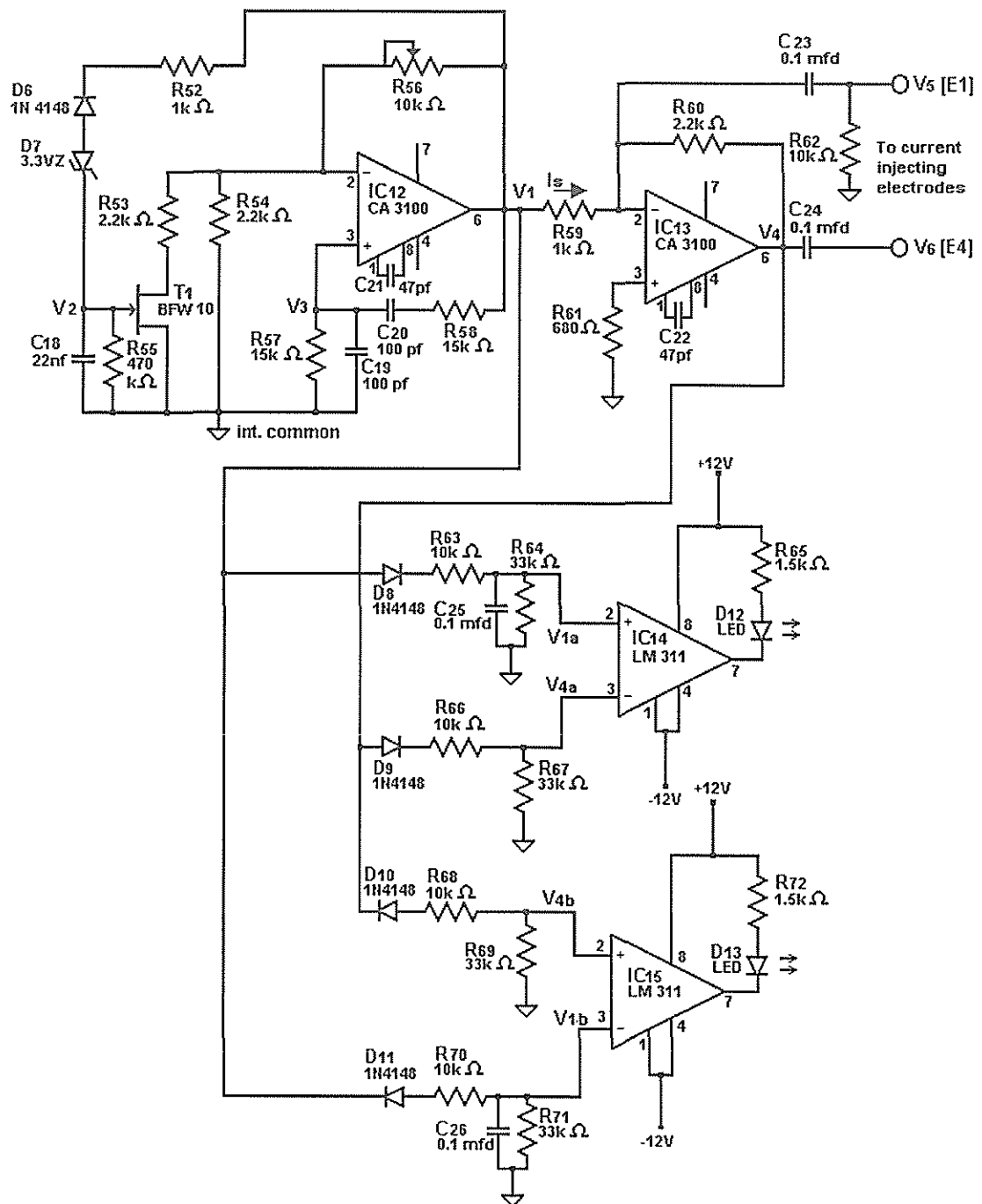
Fig. 4.4 Circuit diagram of oscillator, V-I converter and contact impedance indicator

44
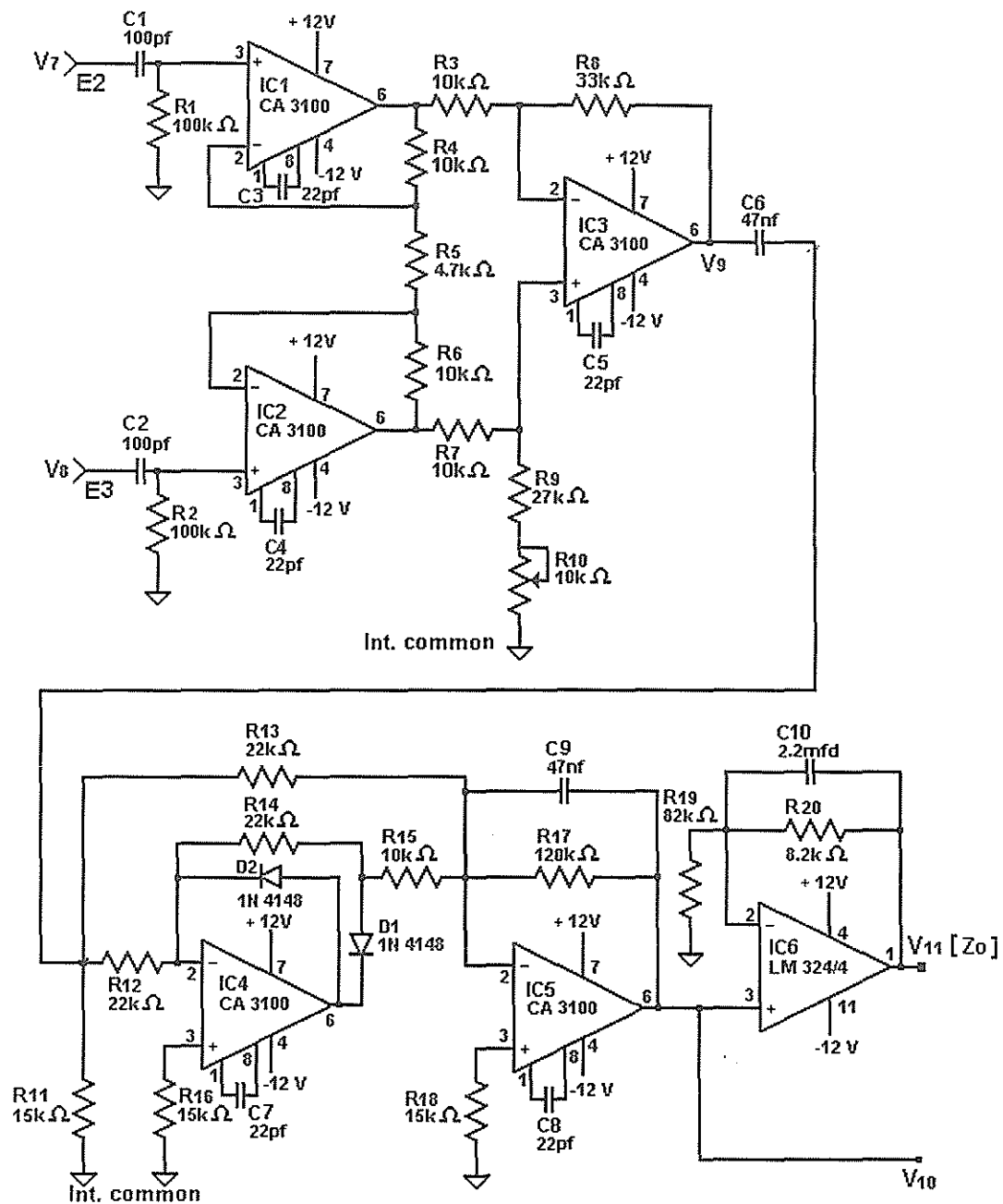
Fig.4.5 Circuit diagram of Instrumentation amplifier,
Demodulator & Zo filter for ICG extraction

45
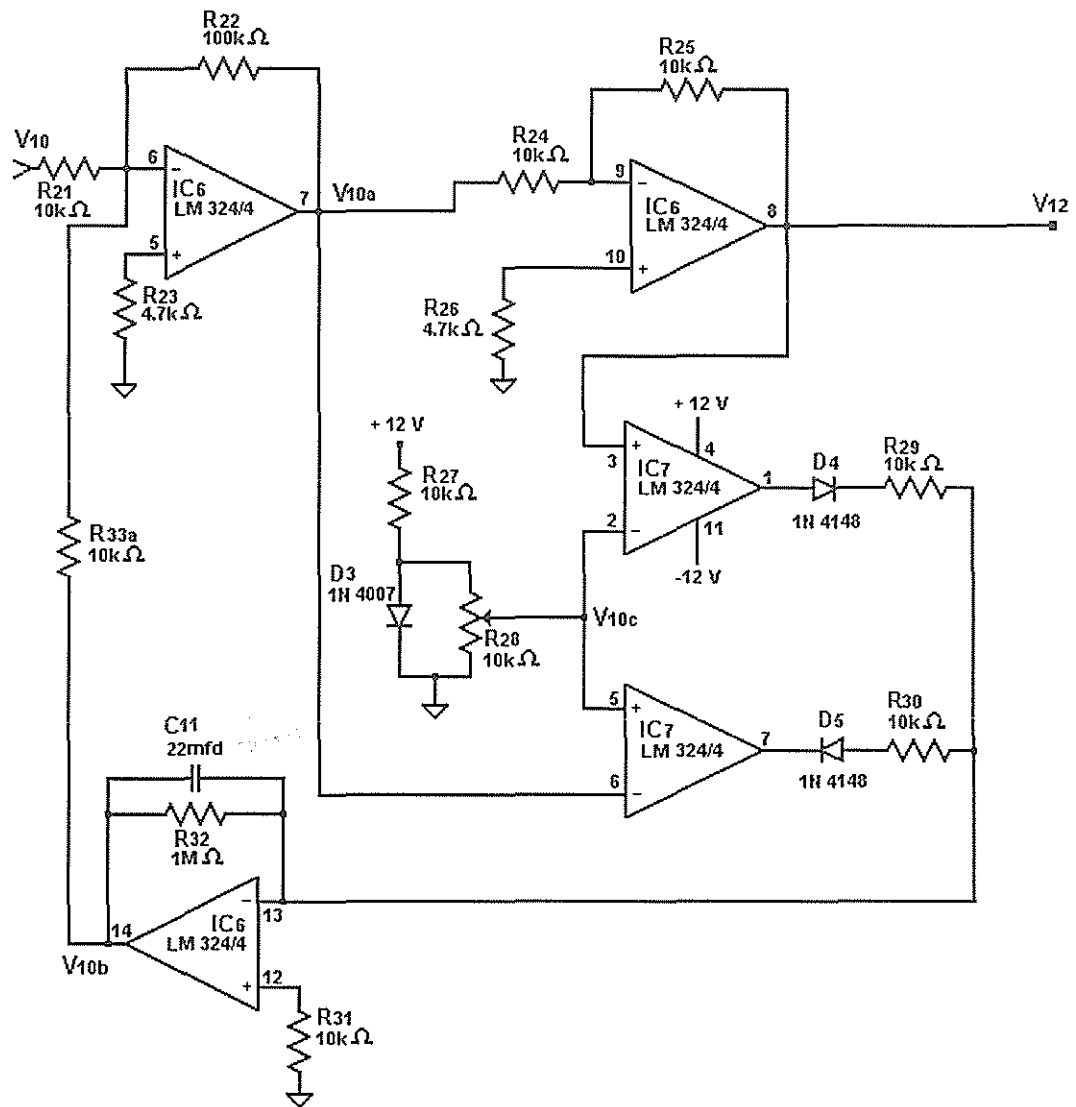
Fig. 4.6  Circuit diagram for DC cancellation

46
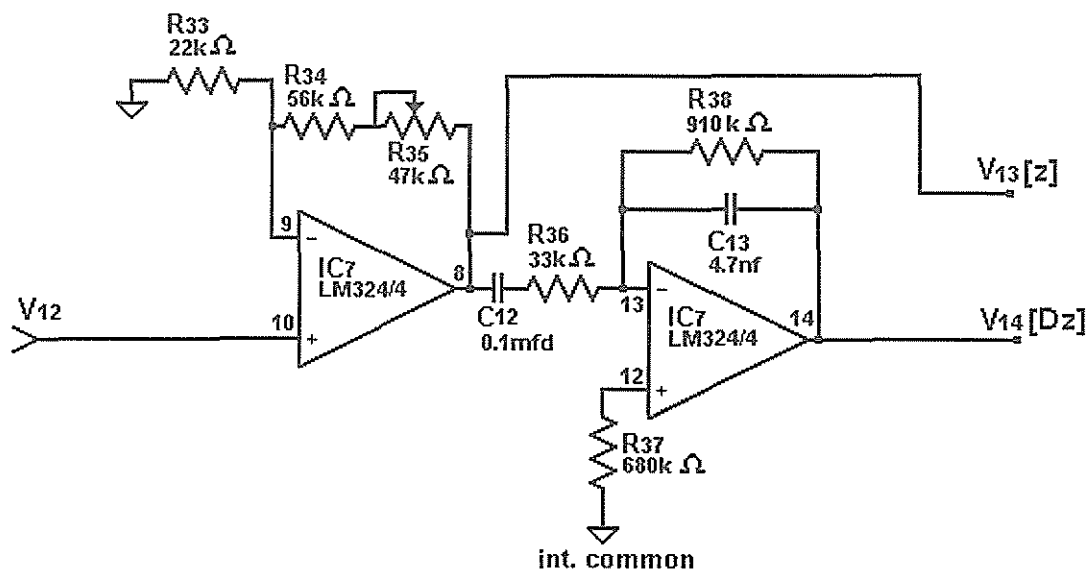
Fig 4.7 z(t) amplifier and Differentiator circuit
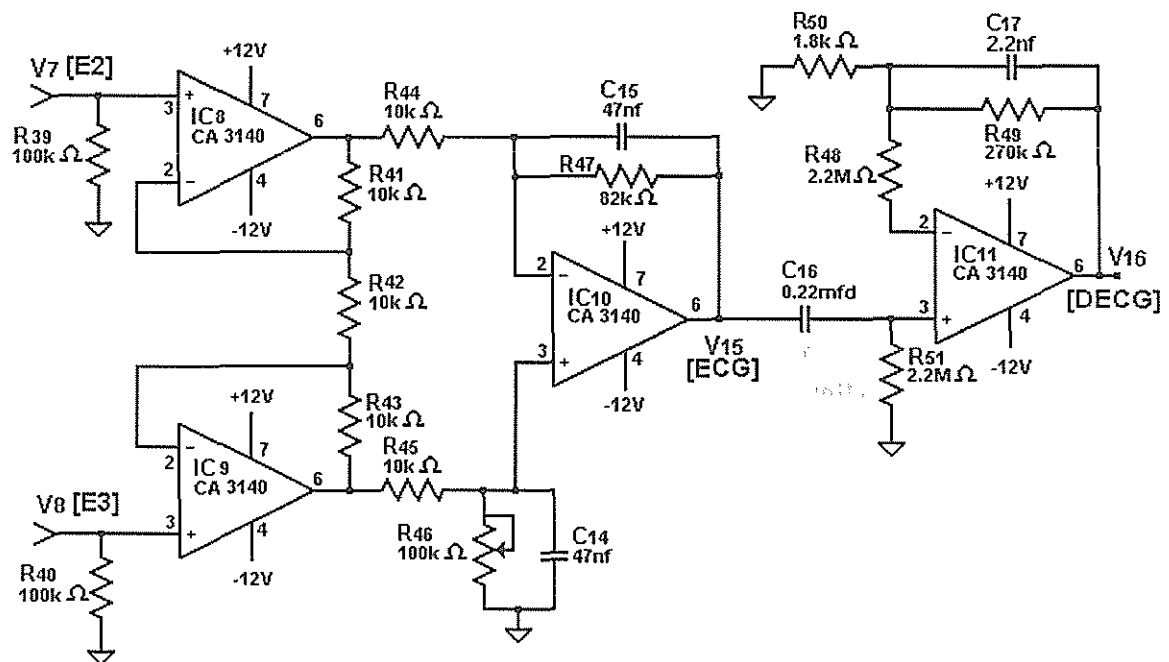


Fig. 4.8 Circuit diagram of ECG instrumentation amplifier and differentiator

47
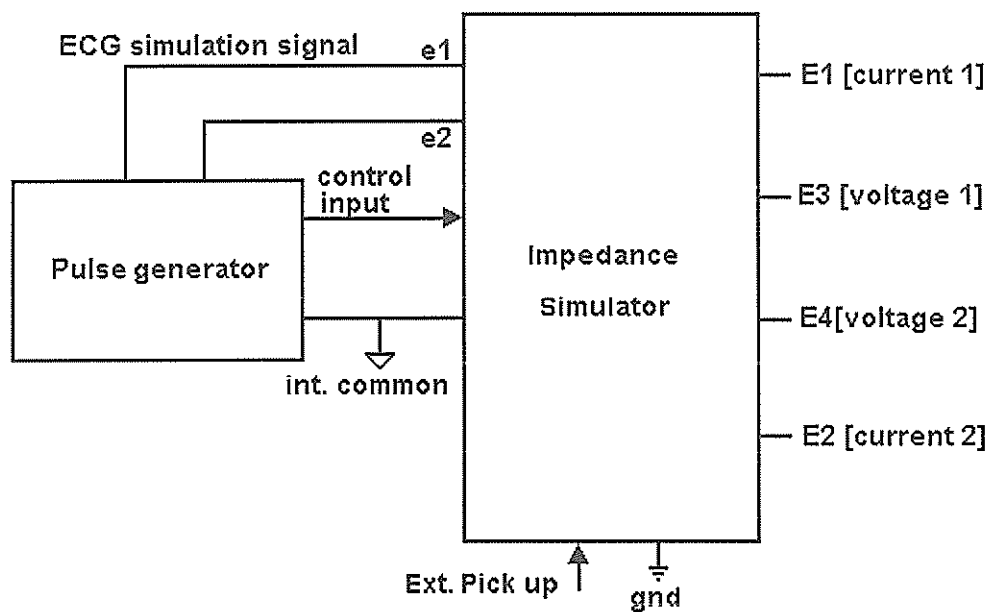
Fig. 4.9  Thorax simulator- block schematic
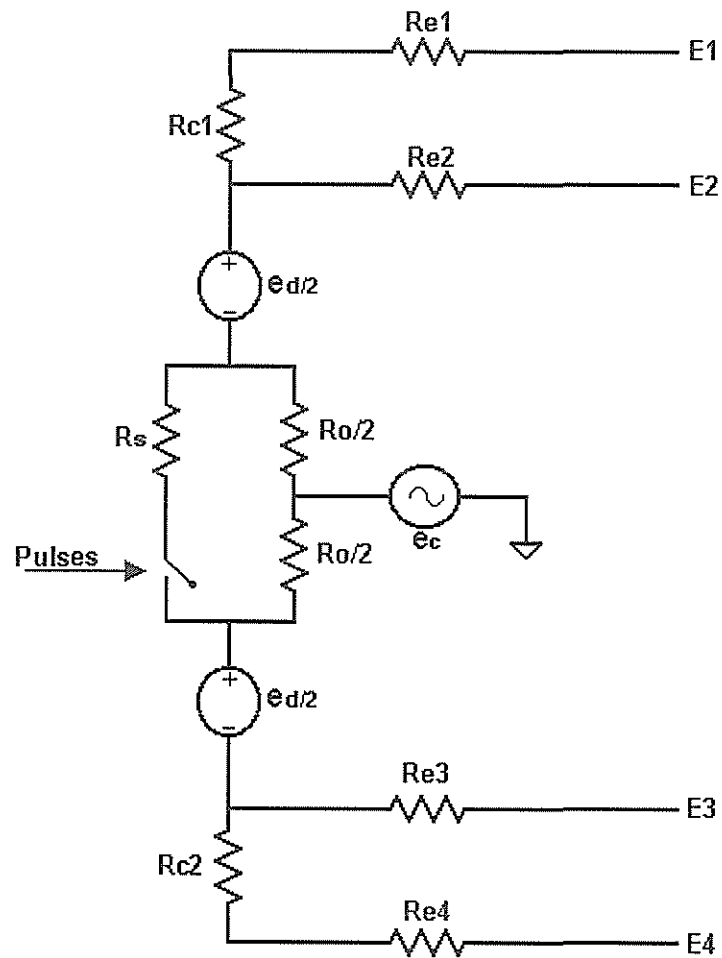
Fig 4.10 Resistive network for thorax simulator

49
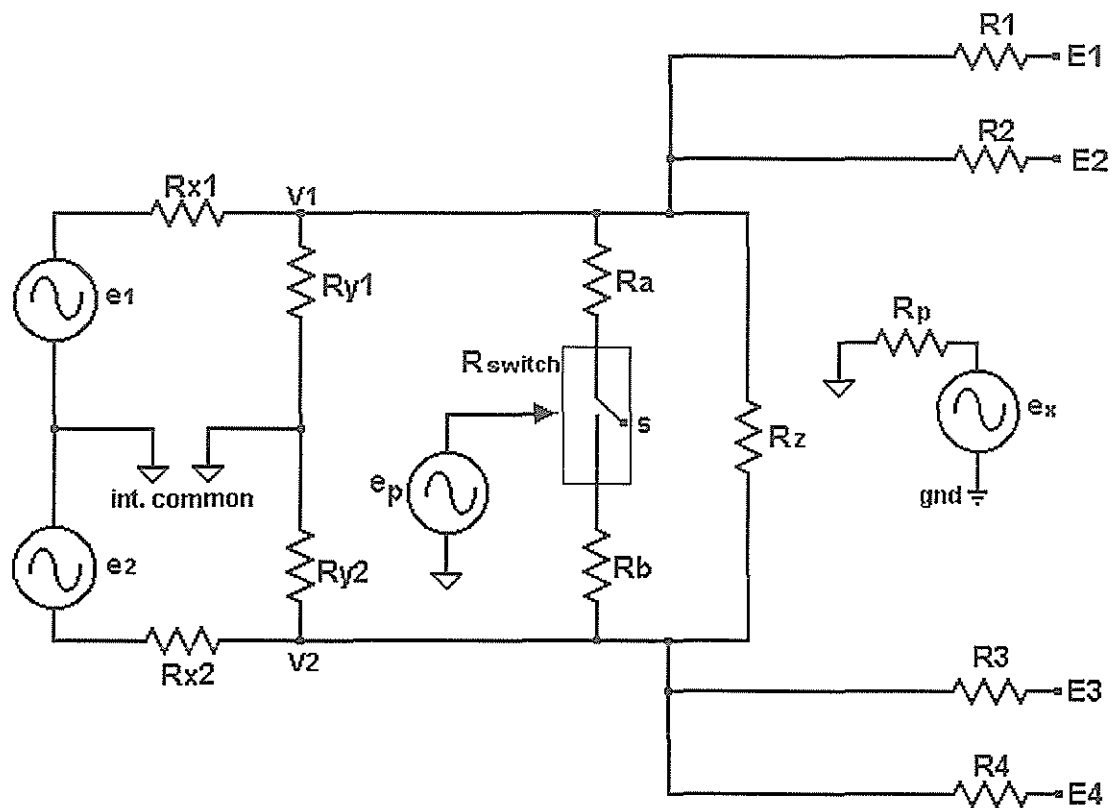
$R_{c1} + R_{e1} = R_1$

$R_{e2} = R_2$

$R_{e3} = R_3$

$R_{e4} + R_{c2} = R_4$

$e_c = \dfrac{V_1 + V_2}{2}$

$e_d = V_1 - V_2$

$R_{y1}' = R_{y1} \| (R_z + (R_{y2} \| R_{x2}))$

$R_{y2}' = R_{y2} \| (R_z + (R_{y1} \| R_{x1}))$

$V_2 = \dfrac{R_{y2}'}{R_{x2} + R_{y2}'} e_2 \qquad V_1 = \dfrac{R_{y1}'}{R_{x1} + R_{y1}'} e_1$

Fig 4.11  Schematic implementation of thoracic impedance simulator as given in Fig 4.10

50
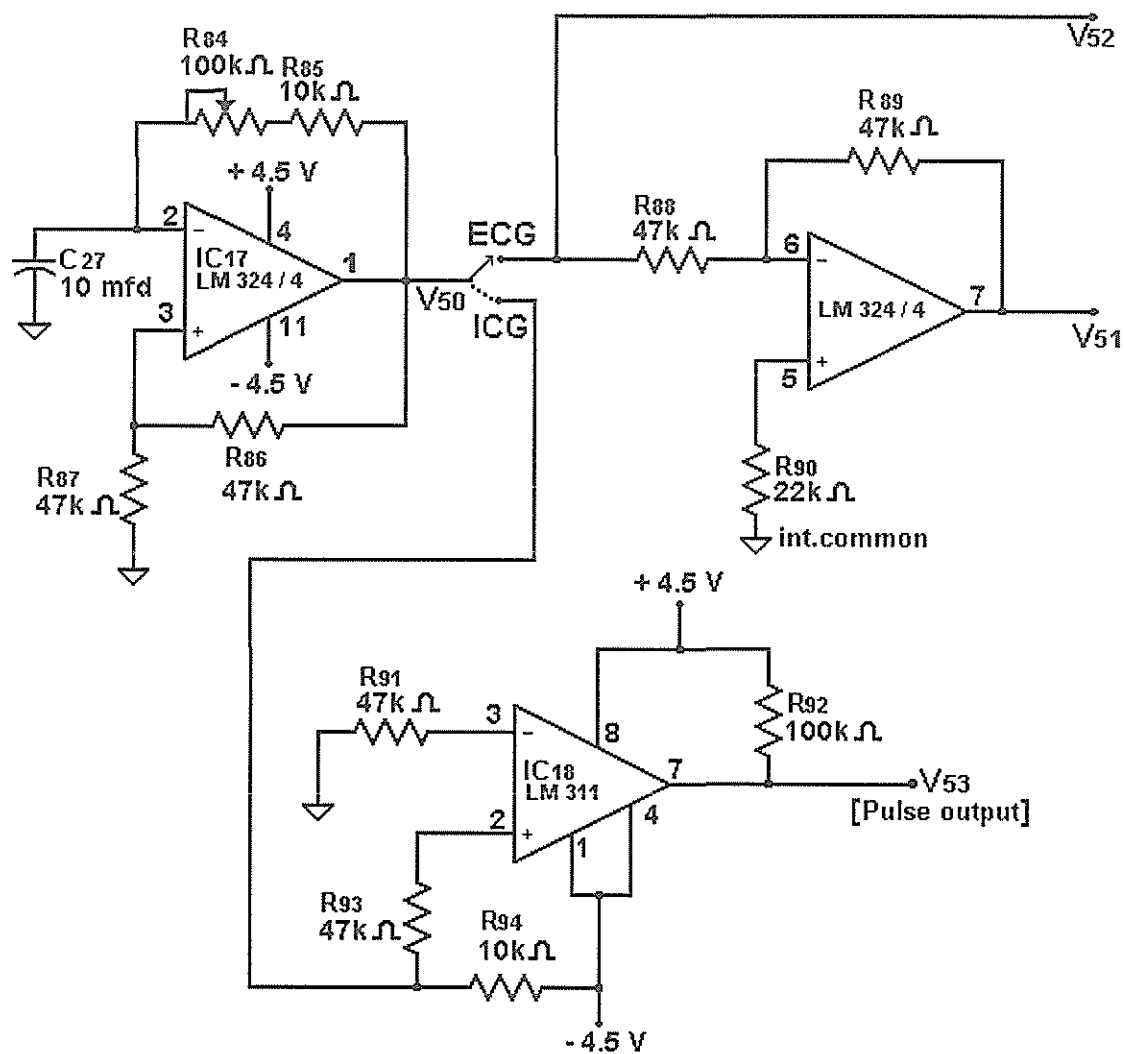
Fig. 4.12   Circuit diagram for ECG simulator and
pulse circuit  for impedance simulator
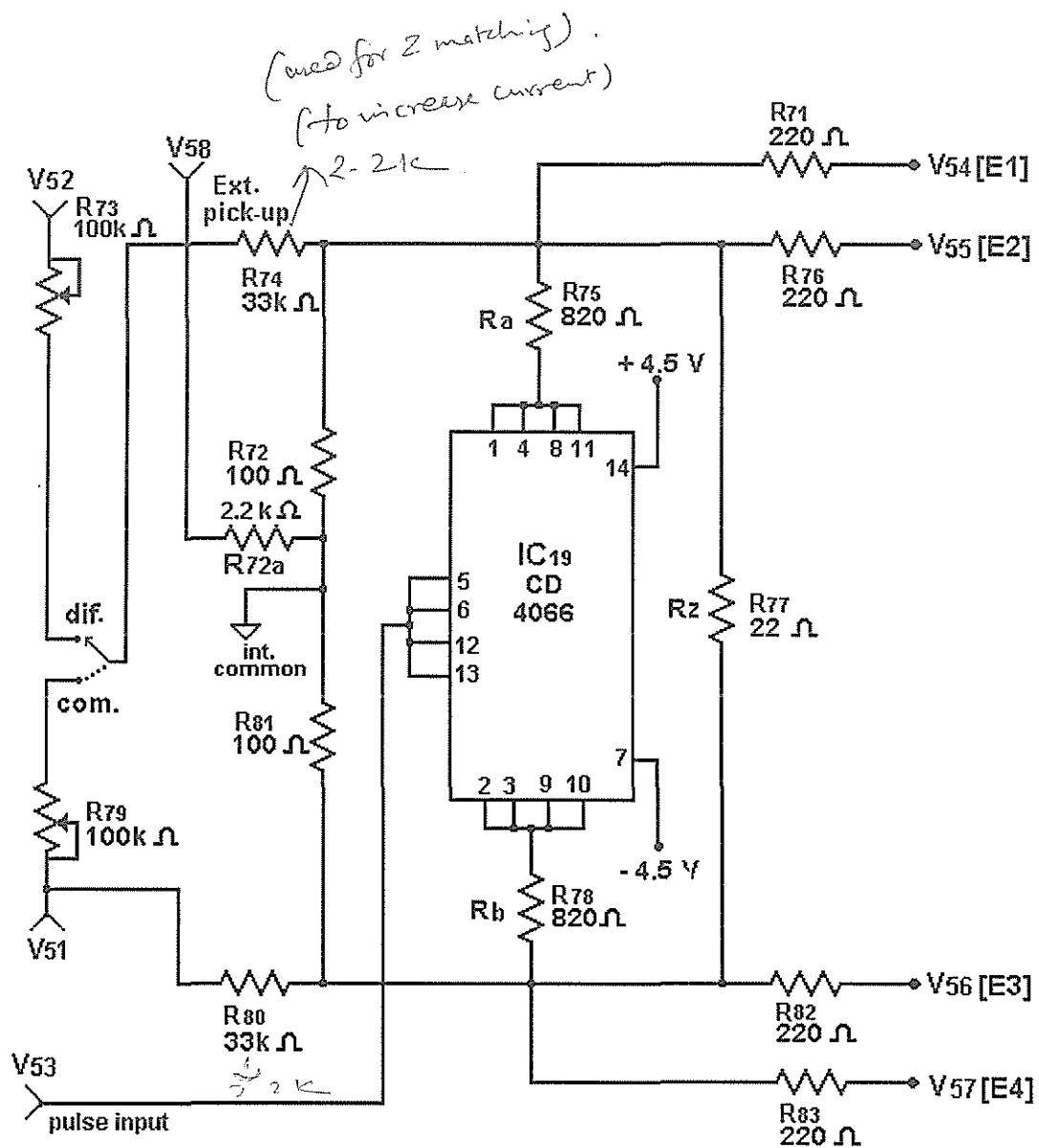
Fig 4.13 Circuit diagram for thoracic impedance simulator
for the schematic shown in Fig 4.11
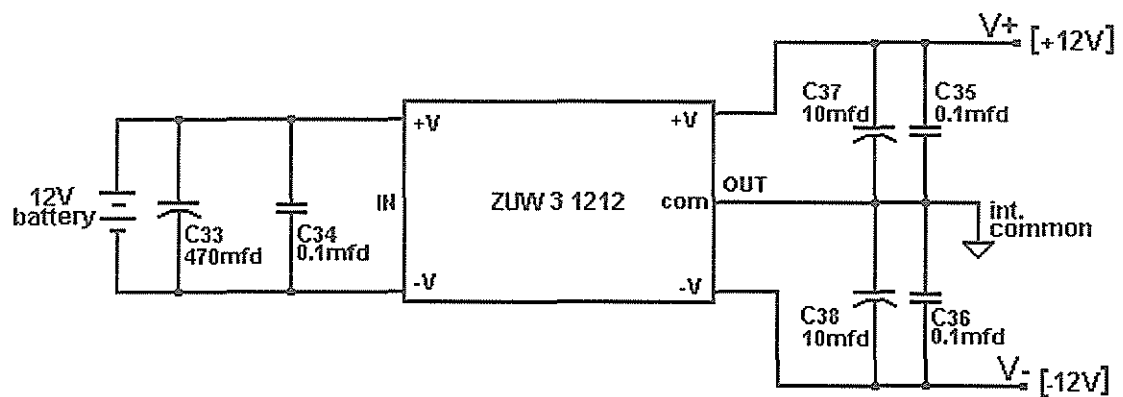
Fig 4.14 Circuit diagram of ICG power supply
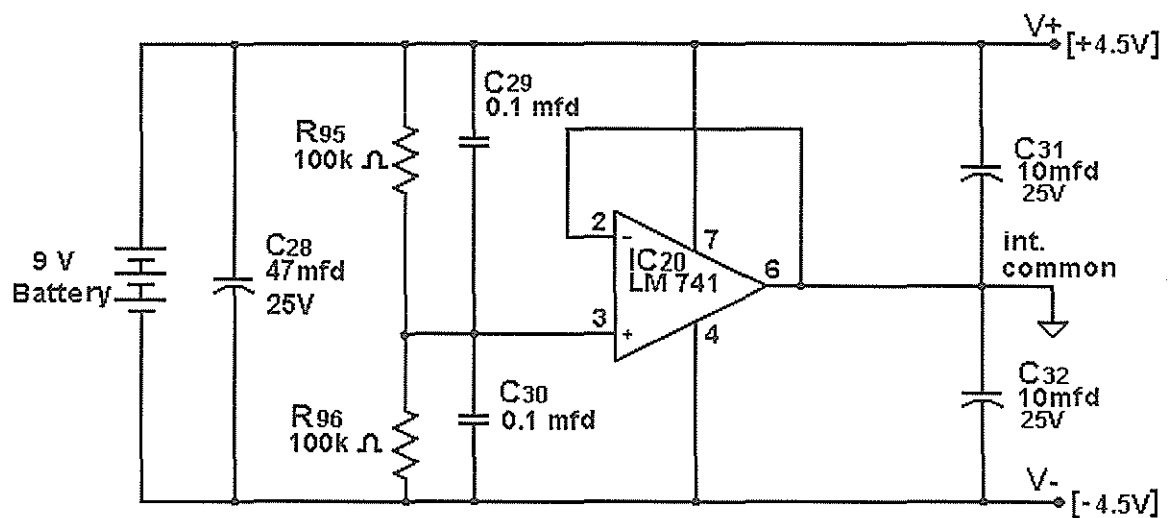


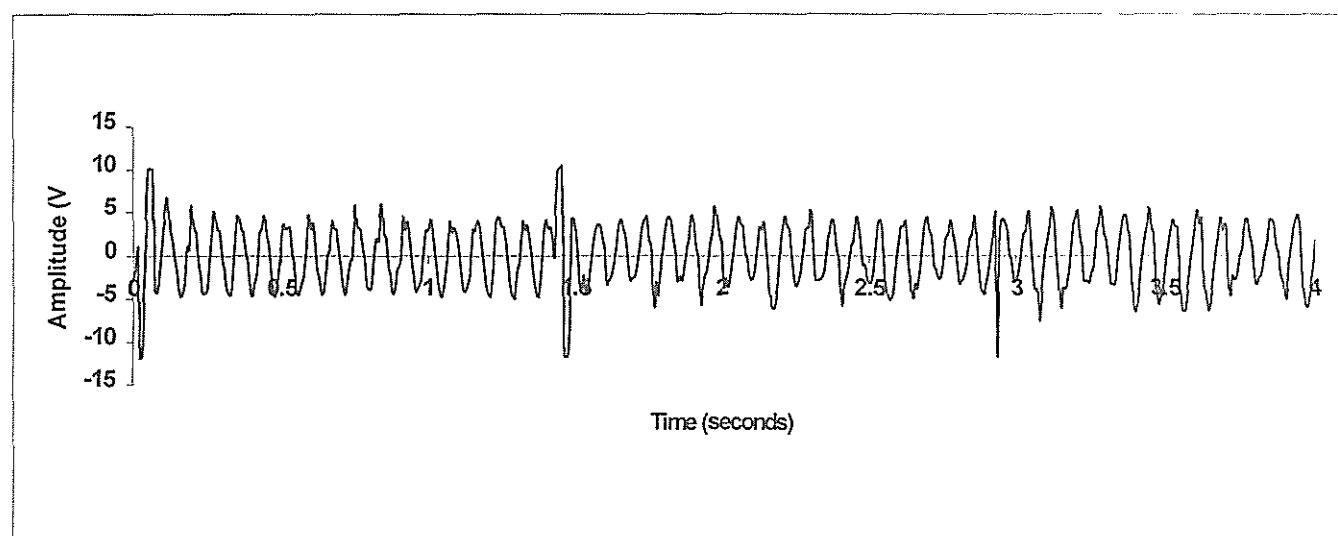Fig 4.15 Circuit diagram of split supply used in simulator

53
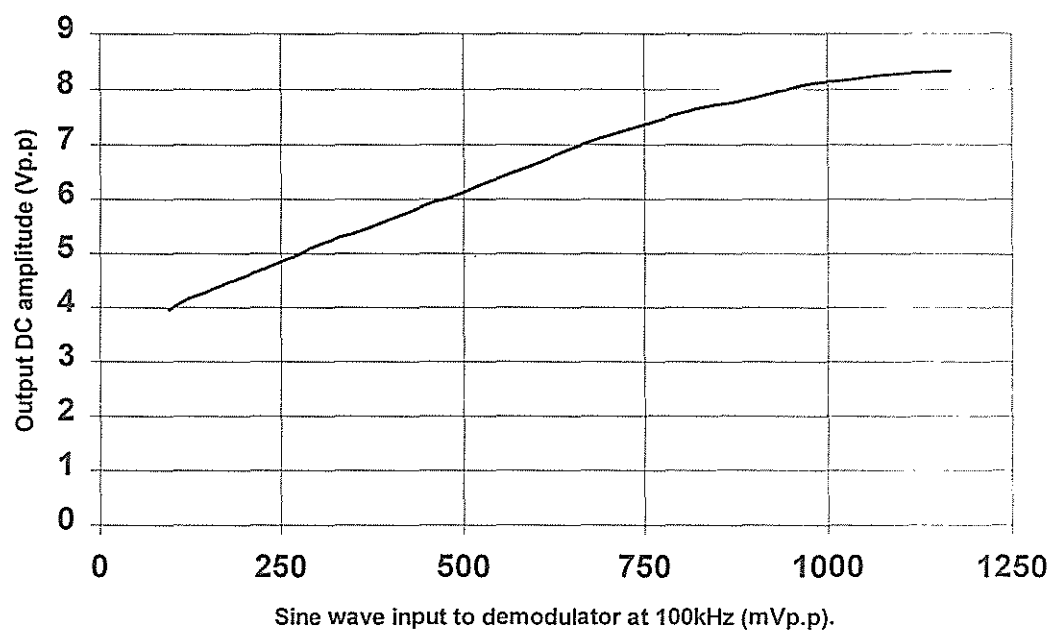
**Fig 5.1 Linearity curve of demodulator in ICG extraction circuit**
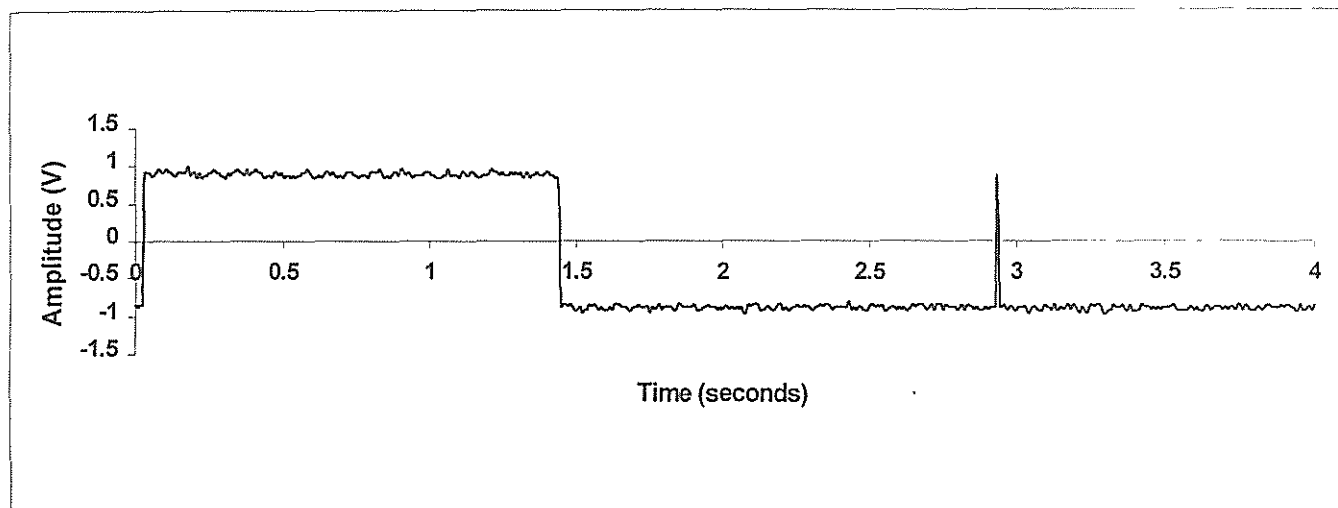
(a)



(b)

Fig 5.2   a. Input to DC cancellation circuit.
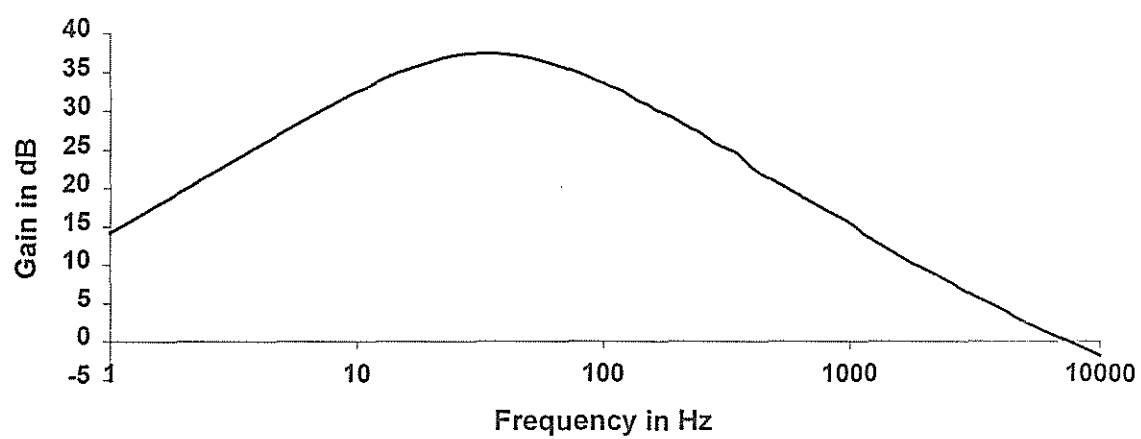
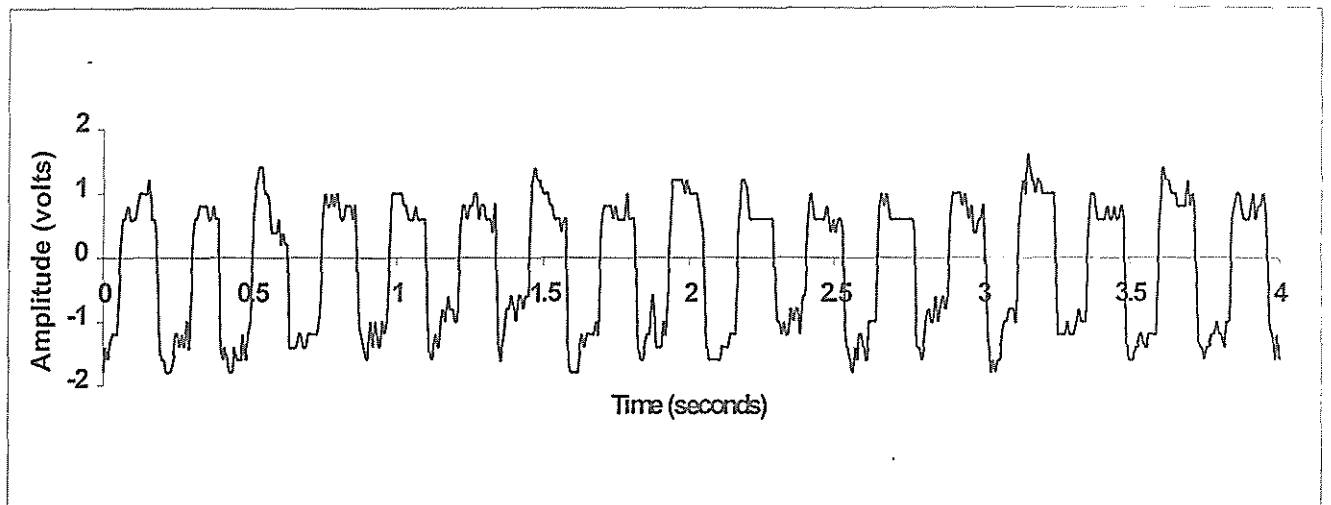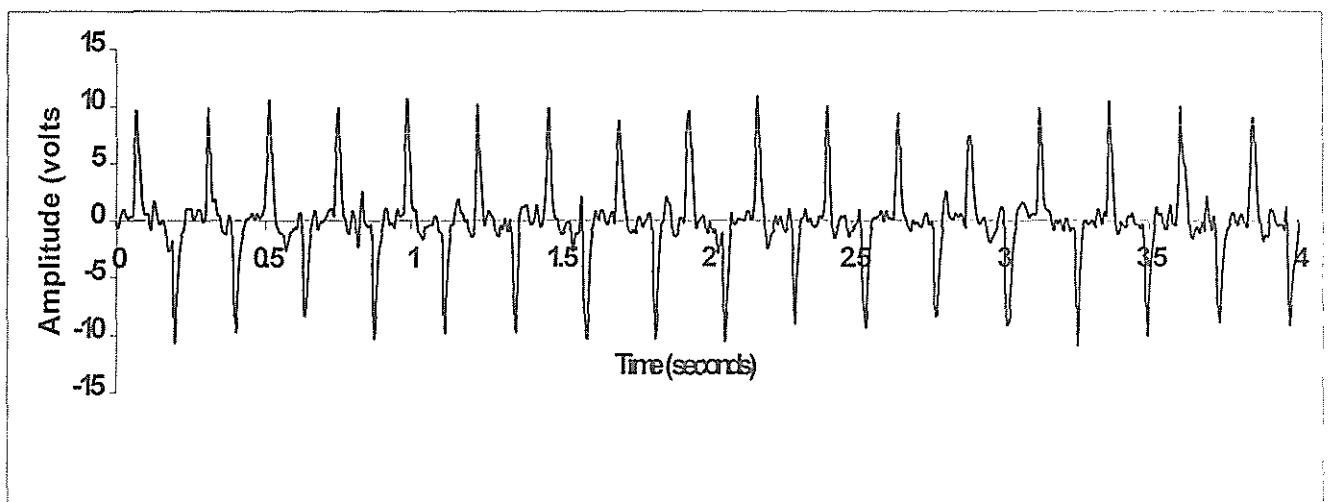b. Output of differentiator connected to DC cancellation circuit

Fig 5.3   Frequency response of *dz(t)/dt* circuit in Fig 4.7

(a)



(b)

Fig 5.4  a. Simulated z waveform recorded in ICG instrument

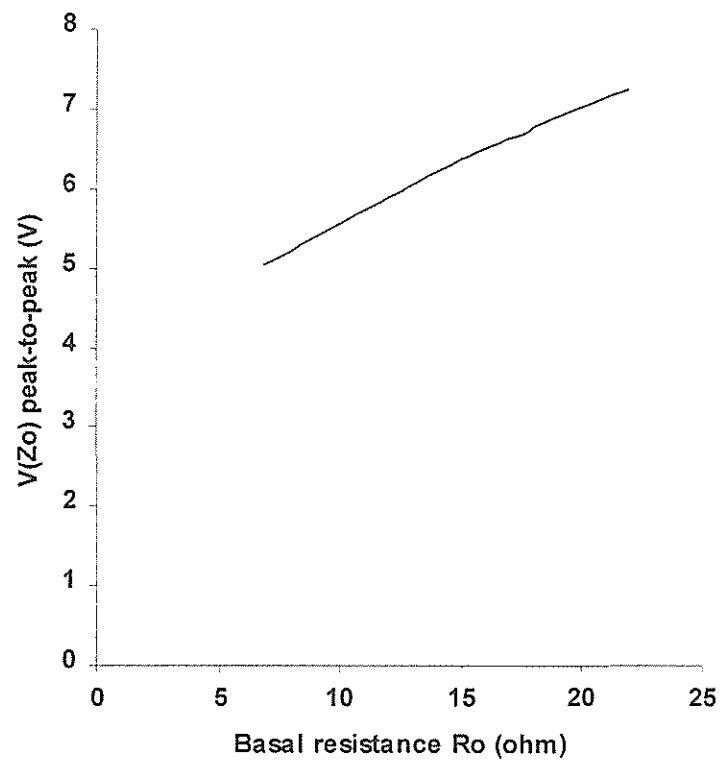b. Simulated dz(t)/dt  waveform recorded from ICG instrument

Fig 5.5  Measured peak-to-peak value of output voltage $Z_o$ for different values of $R_o$(=calculated $R_{off}$) in the simulator
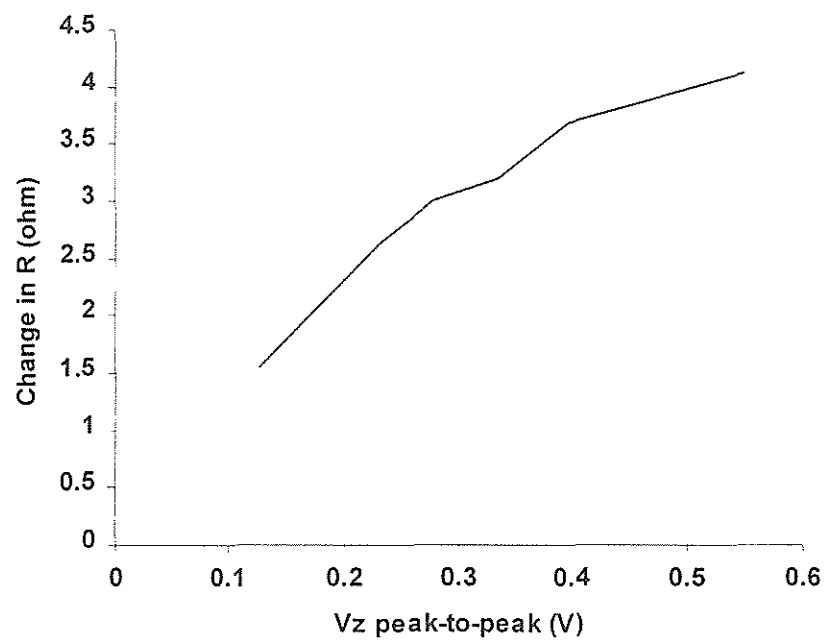
Fig 5.6 Measured peak-to-peak value of output voltage z(t) for different values of ΔR (= calculated $R_{off} - R_{on}$ ) in the simulator
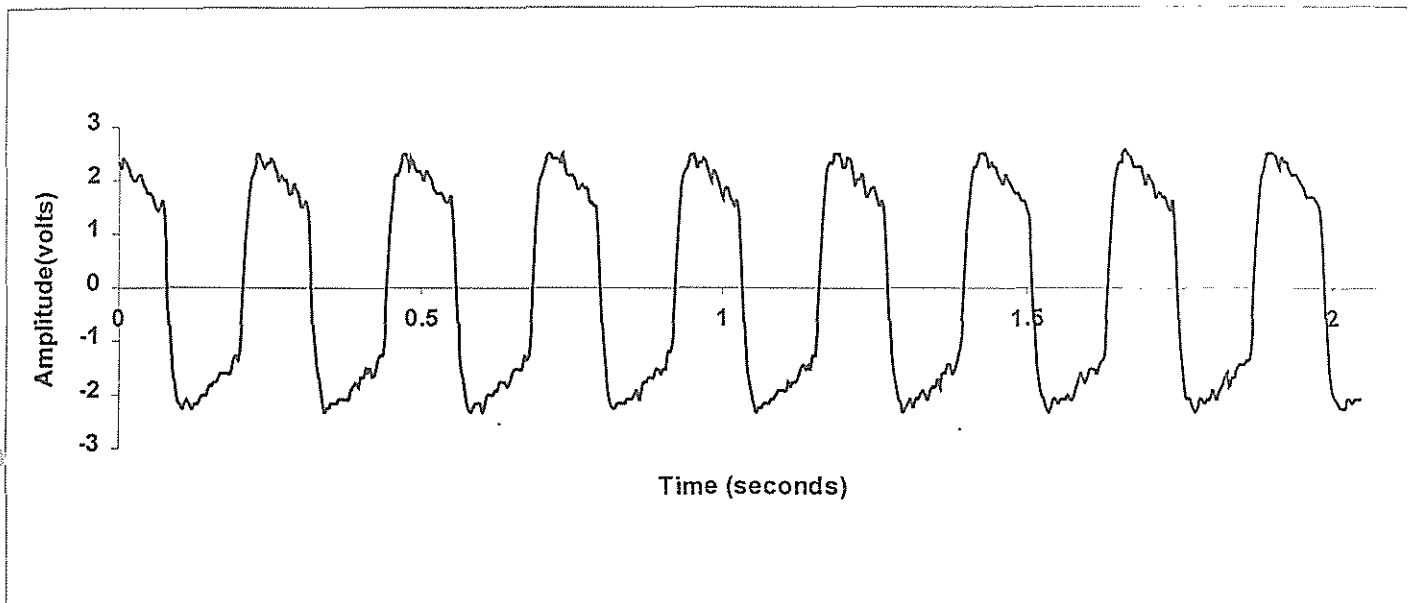
Fig 5.7  Simulated ECG waveform



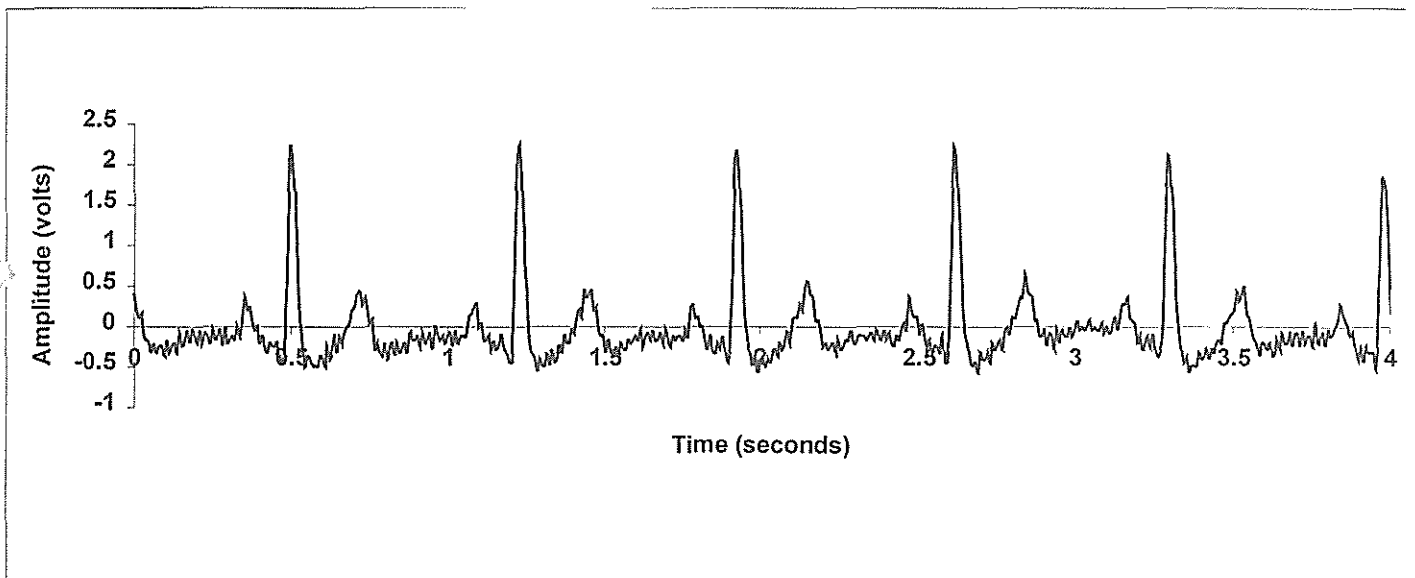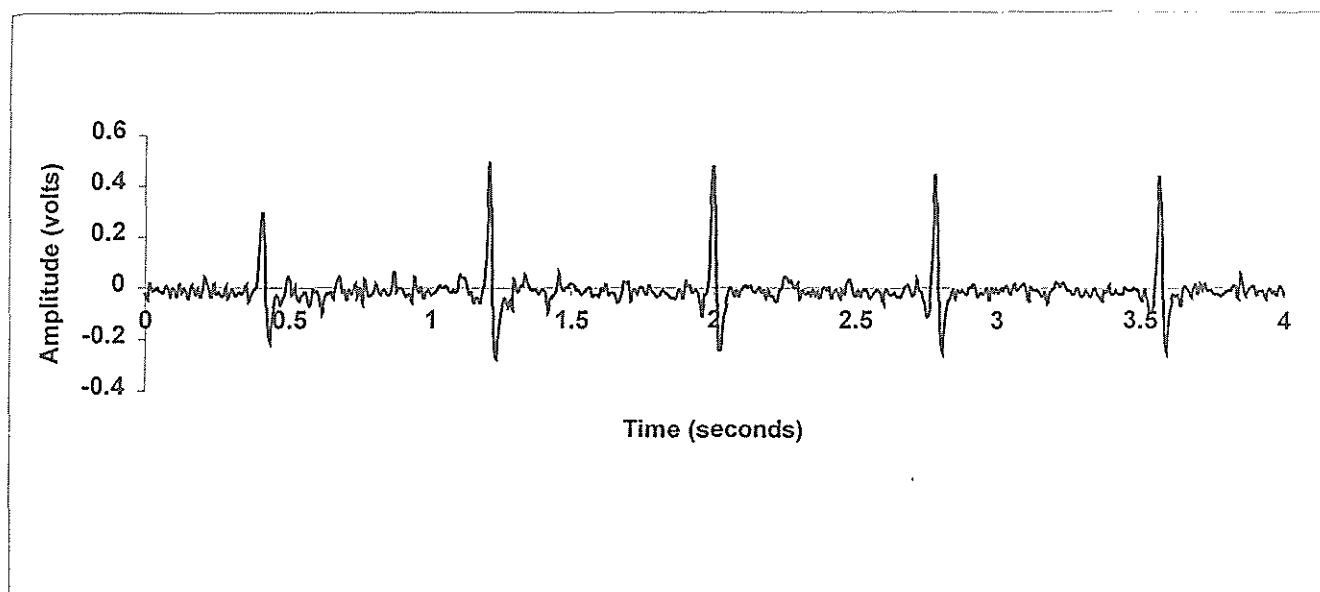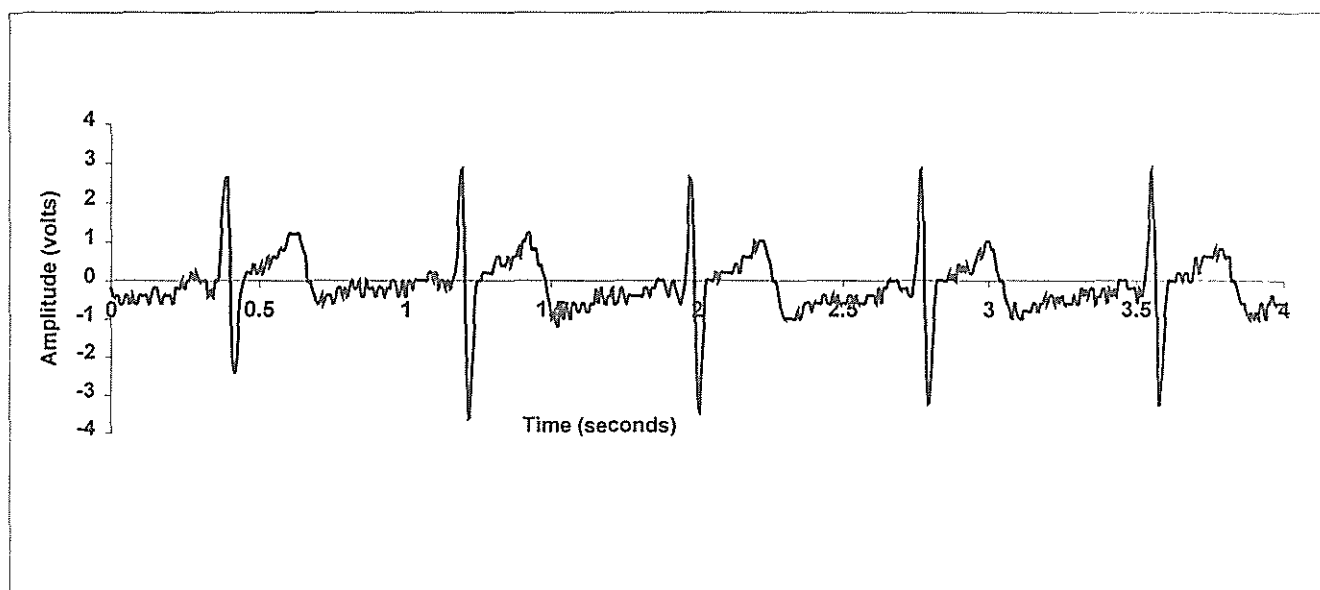Fig 5.8   Recorded d(ECG)/dt from a subject (H. Rate= 87)

60
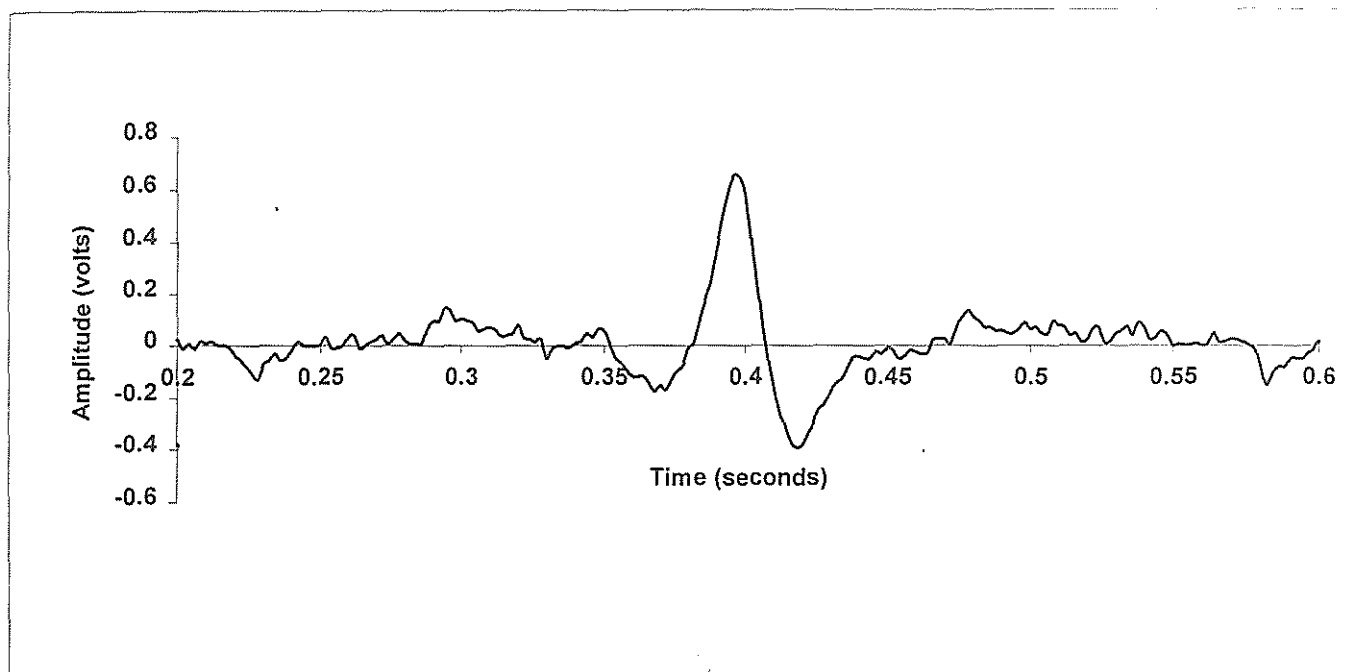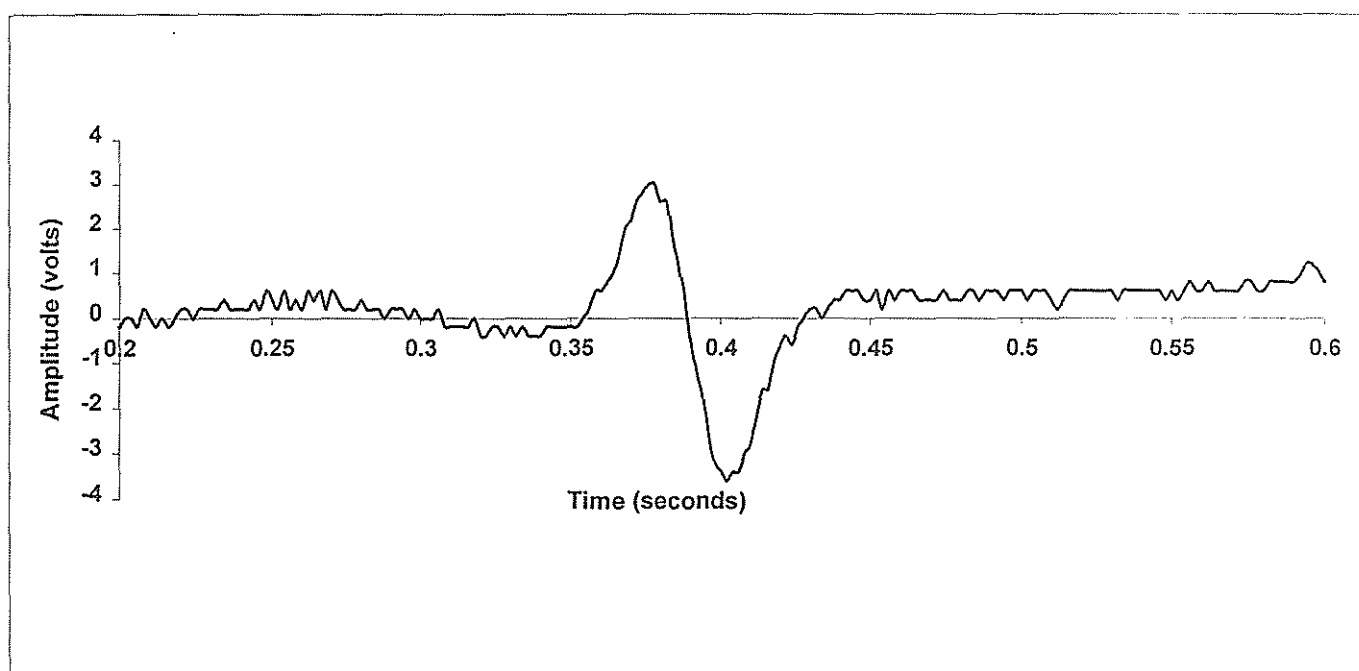
(a)



(b)

Fig 5.9  a. Recorded ICG waveform from ASH

b.  Recorded d(ECG)/dt waveform corr.to (a).

61

(a)



(b)

Fig 5.10   a. Typical ICG recorded from ASH

b. Recorded d(ECG)/dt corr.to ICG in Fig (a)

62

# APPENDIX A

## Balanced current source

At relatively high frequencies, the application of an alternating current through the body or body segment results in electromagnetic stray fields which reduce the amount of actually injected current to the tissue under study. This radiation effect can be reduced by use of a symmetrical current source [15]. The symmetry of such an arrangement depends on the stray capacitances of the source with respect to the surrounding equipment. The asymmetrical configuration introduces a common mode voltage to the measuring input. If the current source is not properly isolated at higher frequencies, stray current will flow through the body due to the generation of electromagnetic field between the body and the ground. Since these stray currents are part of the output delivered by the source, the amount of current flowing in the tissue is reduced. This impairs the accuracy of measurement. The electrical isolation can be obtained by powering the instrument using battery or by floating power sources like DC/DC converters. The main objective is to reduce the leakage currents through the stray capacitances, which connected to ground through the patient. This is of major importance at high frequencies.

If the current source output is a symmetrical circuit, the effect of radiation is further reduced. This is because, the current source provides a virtual zero reference splitting the output voltage into two equal parts of opposite phase. The current carrying cables are to be shielded to reduce the stray capacitances. The zero reference of the isolated section is situated approximately in the center of the impedance under study.

A balanced current source using small transformers with bifilar winding in secondary has been used by Goovaerts, *et al*. As an alternative to this, a balanced current source was devised using op amps alone, i.e. without using transformers. The circuit diagram is shown in Fig A.1. The balanced current source is driven with 100 kHz sinusoidal output of the Wien-bridge oscillator. The current flowing through the tissues under measurement can be set to the appropriate value by designing the value of 'R' at the input of the V-I converter.

63

From the circuit diagram,

Select $R_1 = R_2$, $R_4 = R_5$, $R_3 \approx R_1 \| R_2 \| R_7$, $R_6 \approx R_4 \| R_5$.

$$I_1 = I_2 = I$$

$$V_Z = -V_1 - V_X \qquad (1)$$

$$V_Z = -V_X \qquad (2)$$

$$I = \frac{V_Z - V_Y}{R} \qquad (3)$$

Equation (3) gives $\qquad I = \frac{1}{R}\left(-V_1 - V_X - V_Y\right) = -\frac{V_1}{R} \qquad (4)$

$$V_1 = V_Z - I.R = V_Z + V_1 \qquad (5)$$

The tissue impedance is represented by $R_L$.

Therefore $\qquad V_Y = V_X + I.\ R_L \qquad (6)$

From equations (2) and (6), $\qquad 2.V_X = I.\ R_L$

Thus expression for $V_x$ can be written as

$$V_X = -\frac{1}{2} R_L \cdot \frac{V_1}{R}$$

$$V_Y = \frac{1}{2} R_L \frac{V_1}{R}$$

Therefore $\qquad V_Z = V_1 \left(\frac{R_L}{2.R} - 1\right)$

The circuit shown in Fig A.1 was assembled and executed by sinusoidal input $V_1$ of 100 kHz frequency. Load $R_L = 1$ kΩ. It was found that $V_X(t) = -V_Y(t)$, i.e., the balanced output condition has been verified. For different values of the current setting $R$, the input voltage was adjusted to obtain the same output $V_X$, and they are given in Table A. We see a linear relationship between R and required $V_1$
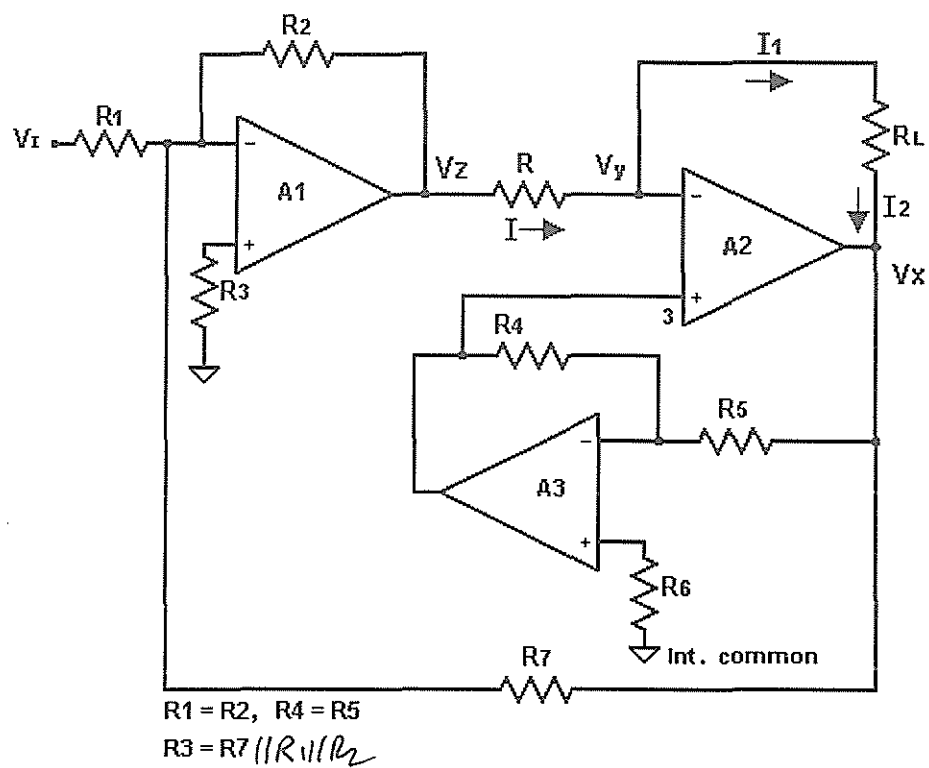
64

R1 = R2,  R4 = R5

R3 = R7 // R1 // R2

**Figure A.1   Balanced Current source circuit using op-amps**

Table A.1   $V_I$ for different $R$, for obtaining $V_X = -V_Y = 1.6$ V

| $R$ ($\Omega$) | $V_I$ (V) |
|:---:|:---:|
| 100 | 0.32 |
| 120 | 0.40 |
| 150 | 0.48 |
| 220 | 0.72 |
| 280 | 0.92 |
| 330 | 1.16 |

# APPENDIX B

## ICG instrument specifications

1. Signal Conditioner

    Power Source      -      12V Battery, 2.5Ah, rechargeable

    Operating current      -      200mA

2. Excitation Circuit

    Excitation frequency      -      100 kHz (fixed)

    Excitation current      -      3 mA rms

3. Electrodes

    Type      -      Suction Cup, non-polarisable

    Material      -      Stainless steel

    Open electrode voltage      -      6.8 $V_{p.p}$, sinusoidal

4. Sensing Circuit

The signal conditioner unit gives four outputs namely $d(ECG)/dt$, $z(t)$, $dz(t)/dt$ and $Z_0$.

    Sensitivity = 10 mV/m$\Omega$

$$\left(\frac{dz}{dt}\right)_{max} = 440mV \equiv 7.62\Omega/s$$

$$Z_0 = 6.850\ V \equiv 20\ \Omega$$

$$d(ECG)/dt = 3\ V_{p.p}$$

# APPENDIX C

## Thorax simulator specifications

1. Power requirements

    DC source :     9 V rechargeable battery

    Supply current :     10 mA approx.

2. Electrical parameters

    $\Delta R$ variation :     $0.1 \, \Omega$ to $0.4 \, \Omega$

    $(0.232 \, \Omega$ typical)

    *ECG* variation :

    common mode :     5– 20 mV

    difference mode :     5– 50 mV

    *ECG/ICG* time control :     0.2 to 2.4 seconds

# APPENDIX D

## List of components used for ICG instrument and Thorax simulator

| Component designator | Part description | Component specification | Approx. price/unit Rs). |
|---|---|---|---|
| R1,R2,R22,R39, R40,R92,R95,R96 | Resistor | 100kΩ,¼w | 0.20 |
| R3,R4,R6,R7,R15, R21,R24,R25,R27, R29,R30,R31,R62 R33a,R63,R66,R68, R70,R85,R94 | Resistor | 10kΩ,¼w | 0.20 |
| R5,R23,R26 | Resistor | 4.7kΩ,¼w | 0.20 |
| R8,R36,R64,R67, R69,R71,R74,R80 | Resistor | 33kΩ,¼ w | 0.20 |
| R9 | Resistor | 27kΩ,¼w | 0.20 |
| R11,R16,R18,R57, R58 | Resistor | 15kΩ, ¼w | 0.20 |
| R12,R13,R14,R33, R90 | Resistor | 22kΩ,¼w | 0.20 |
| R17 | Resistor | 120kΩ,¼w | 0.20 |
| R19,R47 | Resistor | 82kΩ,¼w | 0.20 |
| R20 | Resistor | 8.2kΩ,¼w | 0.20 |
| R32 | Resistor | 1MΩ,¼w | 0.20 |
| R34 | Resistor | 56kΩ,¼w | 0.20 |
| R37,R38 | Resistor | 68kΩ,¼w | 0.20 |
| R48,R51 | Resistor | 2.2MΩ,¼w | 0.20 |
| R49 | Resistor | 270kΩ,¼w | 0.20 |
| R50 | Resistor | 1.8kΩ,¼w | 0.20 |
| R52,R59 | Resistor | 1kΩ,¼w | 0.20 |
| R53,R54,R60 | Resistor | 2.2kΩ,¼w | 0.20 |
| R55 | Resistor | 470kΩ,¼w | 0.20 |
| R61 | Resistor | 680Ω,¼w | 0.20 |
| R65,R72 | Resistor | 1.5kΩ,¼w | 0.20 |
| R71,R76,R82,R83 | Resistor | 220Ω,¼w | 0.20 |
| R72,R81 | Resistor | 100Ω¼,w | 0.20 |
| R77 | Resistor | 22Ω,¼w | 0.20 |
| R86,R87,R88,R89, R91,R93 | Resistor | 47kΩ¼,w | 0.20 |
| R10,R28,R56 | Potentiometer | 10kΩ,cermet | 30.00 |
| R35 | Potentiometer | 47kΩ,cermet | 30.00 |
| R46 | Potentiometer | 100kΩ,cermet | 30.00 |

| Component designator | Part description | Component specification | Approx. price/unit Rs). |
|---|---|---|---|
| R10,R28,R56 | Potentiometer | 10kΩ,cermet | 30.00 |
| R35 | Potentiometer | 47kΩ,cermet | 30.00 |
| R46 | Potentiometer | 100kΩ,cermet | 30.00 |
| R73,R79,R84 | Potentiometer | 100kΩ,carbon | 10.00 |
| C1,C2,C19,C20 | Ceramic disc capacitor | 100pF,25V | 1.00 |
| C3,C4,C5,C7,C8, C21,C22 | Ceramic disc capacitor | 22pF,25V | 1.00 |
| C13 | Ceramic disc capacitor | 4.7nF,25V | 1.00 |
| C6,C9,C14,C15 | Ceramic disc capacitor | 47nF,25V | 1.00 |
| C10 | Electrolytic | 2.2μF,25V | 1.50 |
| C11 | Electrolytic | 22μF,25V | 2.00 |
| C12,C23,C24,C25, C26,C29,C30 | Ceramic disc capacitor | 0.1μF,25V | 1.00 |
| C16 | Ceramic disc capacitor | 0.22μF,25V | 1.00 |
| C17 | Ceramic disc capacitor | 2.2nF,25V | 1.00 |
| C18 | Ceramic disc capacitor | 22nF,25V | 1.00 |
| C27,C31,32 | Electrolytic | 10μF,25V | 2.00 |
| C28 | Electrolytic | 47μF,25V | 4.00 |
| D1,D2,D4,D5,D6, D8, D9,D10,D11 | Si switching diode | 1N 4148 | |
| D3 | Si diode | 1N 4007 | 0.75 |
| D7 | Zener diode | 3.3V | 2.00 |
| D12,D13 | LED | Green | 1.50 |
| IC1,IC2,IC3,IC4, IC5,IC12,IC13 | 8 pin DIP | CA3100 | 40.00 |
| IC6,IC7,IC17 | 14 pin DIP | LM324 | 12.00 |
| IC8,IC9,IC10, IC11 | 8 pin DIP | CA3140 | 30.00 |
| IC14,IC15,IC18 | 8 pin DIP | LM311 | 20.00 |
| IC19 | 14 pin DIP | CD 4066 | 45.00 |
| IC 20 | 8 pin DIP | LM 741 | 7.50 |
| T1 | n-channel JFET | BFW10 | 10.00 |
| PCBs | Glass epoxy | Double sided | 600.00 |
| Enclosures | Acrylic | | 300.00 |
| Batteries | rechargeable | 9 V & 12 V | 700.00 |

# APPENDIX E
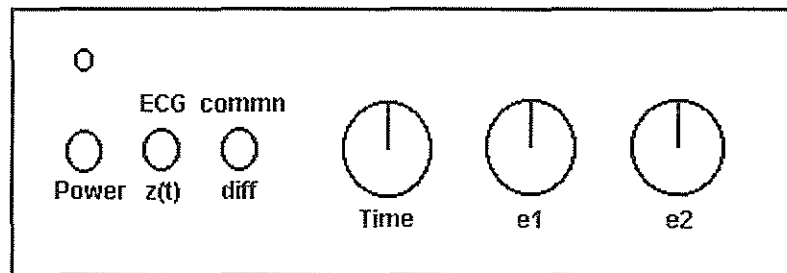
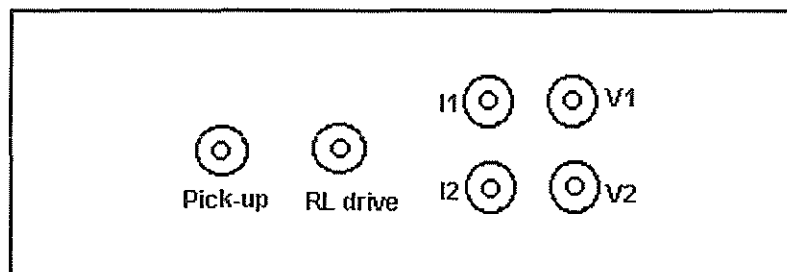Enclosure layout of ICG instrument
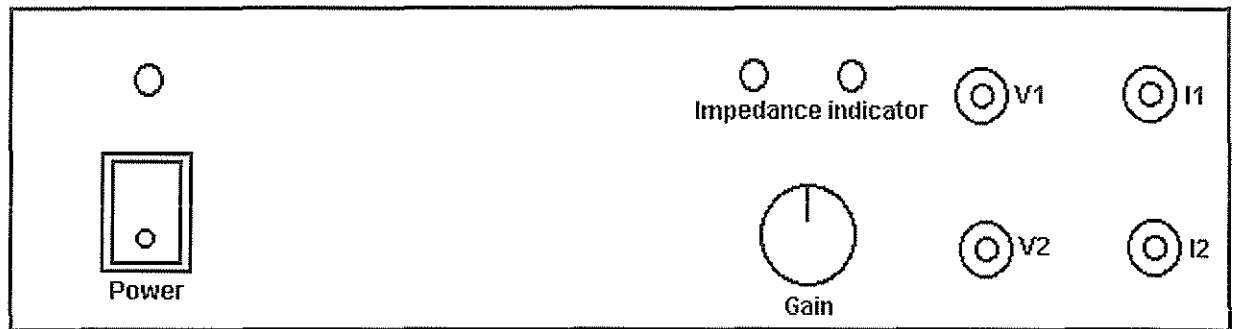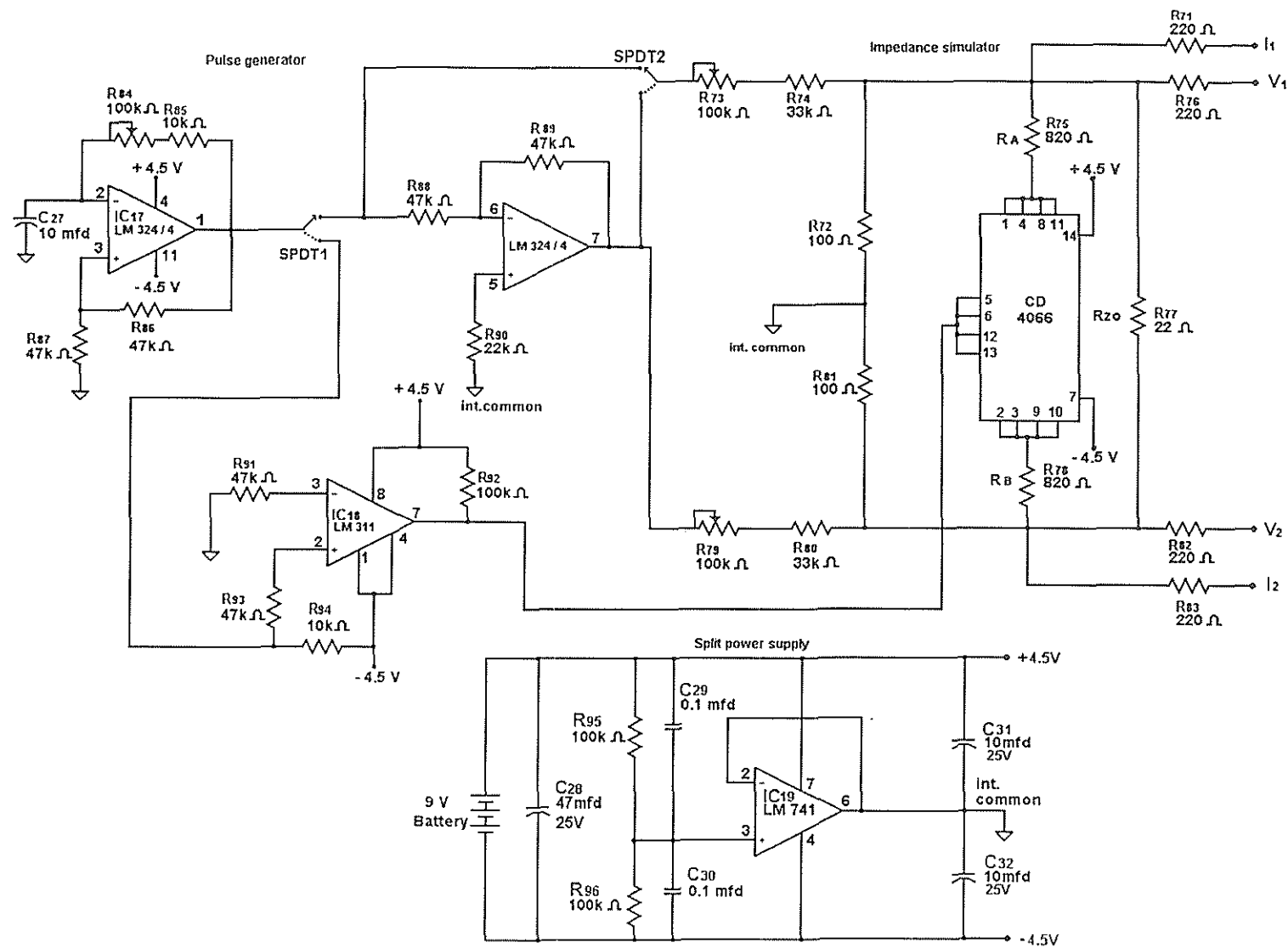


Front panel
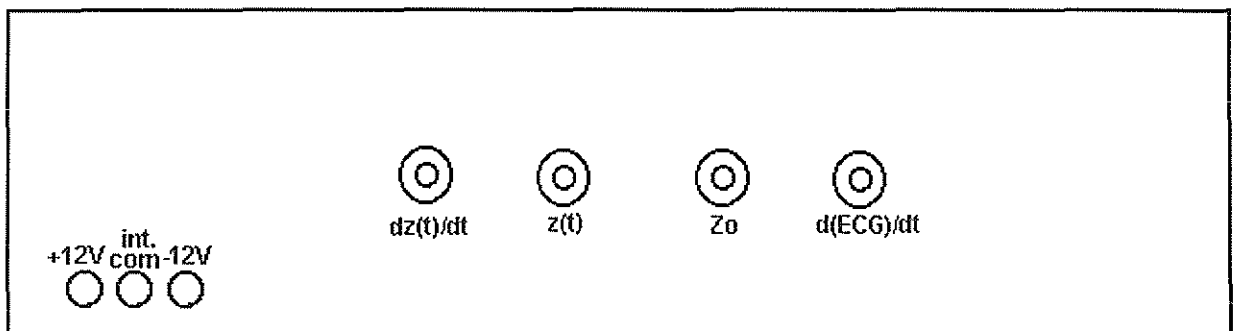


Back panel

# APPENDIX F

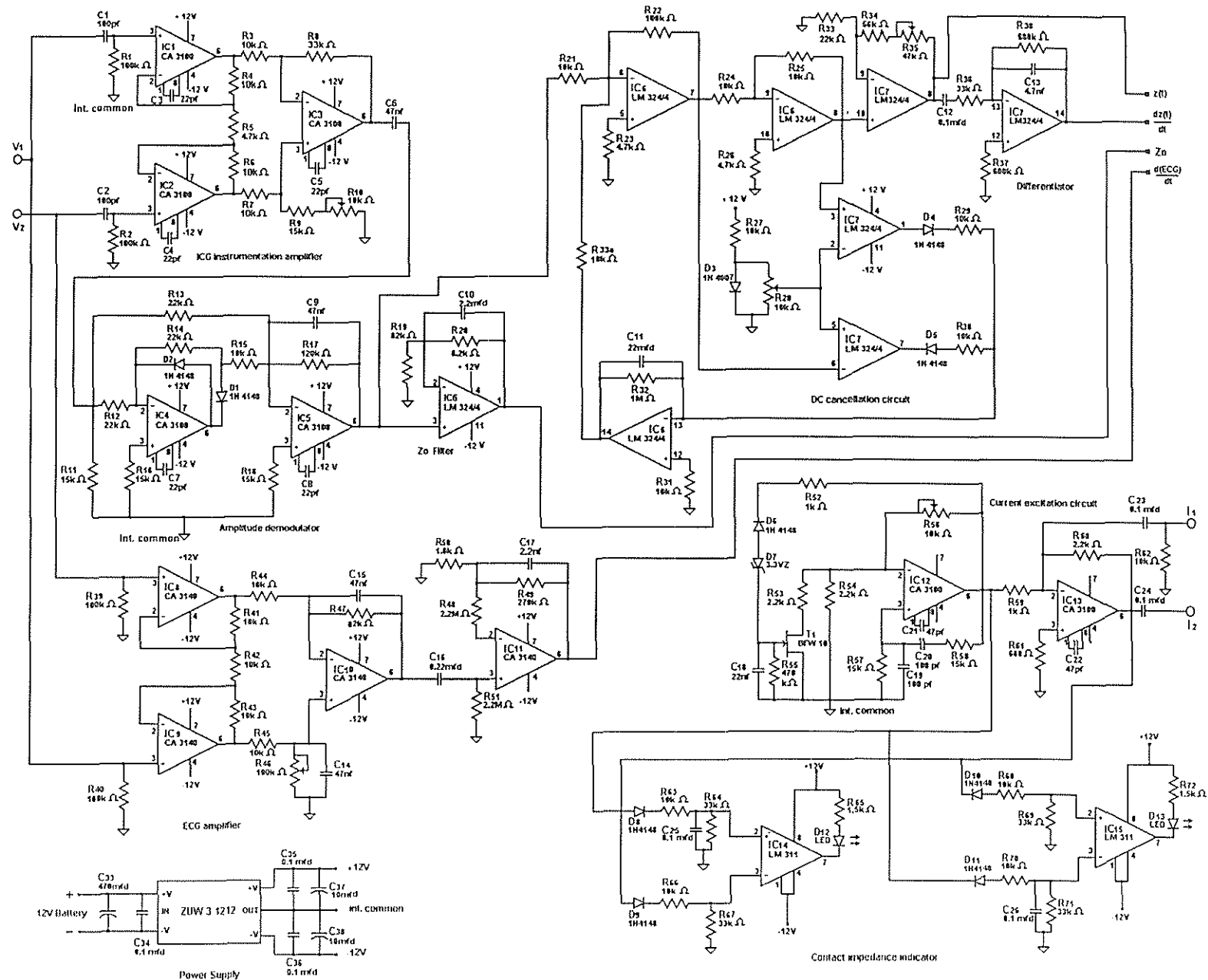Enclosure layout of Thoracic impedance simulator
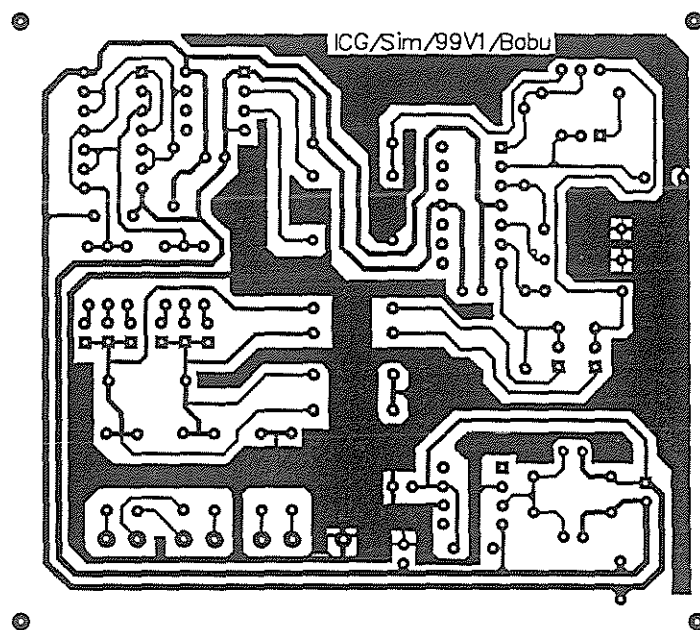


Front panel



Back panel

APPENDIX G

Pulse generator

R84
100kΩ  R85
10kΩ

+4.5 V

2  −
IC17
LM 324/4
3  +

4

1

11

−4.5 V

C27
10 mfd

R87
47kΩ

R86
47kΩ

SPDT1

SPDT2

R89
47kΩ

R88
47kΩ

6  −
LM 324/4
5  +

7

R90
22kΩ

int.common

+4.5 V

R91
47kΩ

3  −
IC18
LM 311
2  +

8

7

4

1

R92
100kΩ

R93
47kΩ

R94
10kΩ

−4.5 V

Impedance simulator

R71
220 Ω

I1

R73
100kΩ

R74
33kΩ

V1

R76
220 Ω

R A    R75
820 Ω

+4.5 V

1  4  8 11      14

5
6
12
13

CD
4066

R72
100 Ω

int. common

R81
100 Ω

Rzo    R77
22 Ω

2  3  9 10      7

−4.5 V

R B    R78
820 Ω

R79
100kΩ

R80
33kΩ

V2

R82
220 Ω

I2

R83
220 Ω

Split power supply

+4.5V

R95
100kΩ

C29
0.1 mfd

9 V
Battery

C28
47mfd
25V

C30
0.1 mfd

2  −
IC19
LM 741
3  +

7

6

4

C31
10mfd
25V

Int.
common

C32
10mfd
25V

R96
100kΩ

−4.5V

Circuit schematic of thorax simulator

Circuit schematic of ICG instrument

# APPENDIX H



ICG/Sim/99V1/Bobu
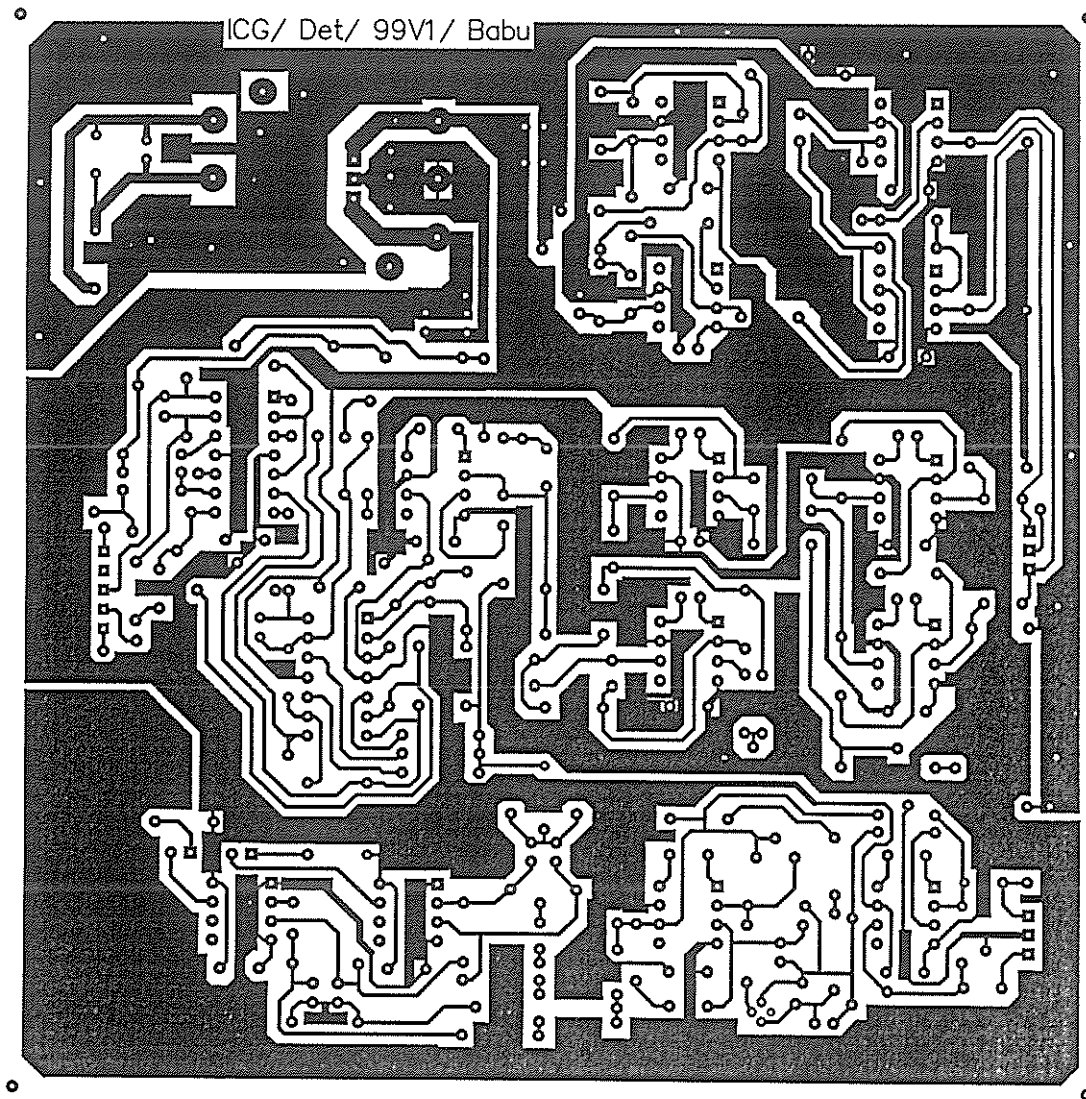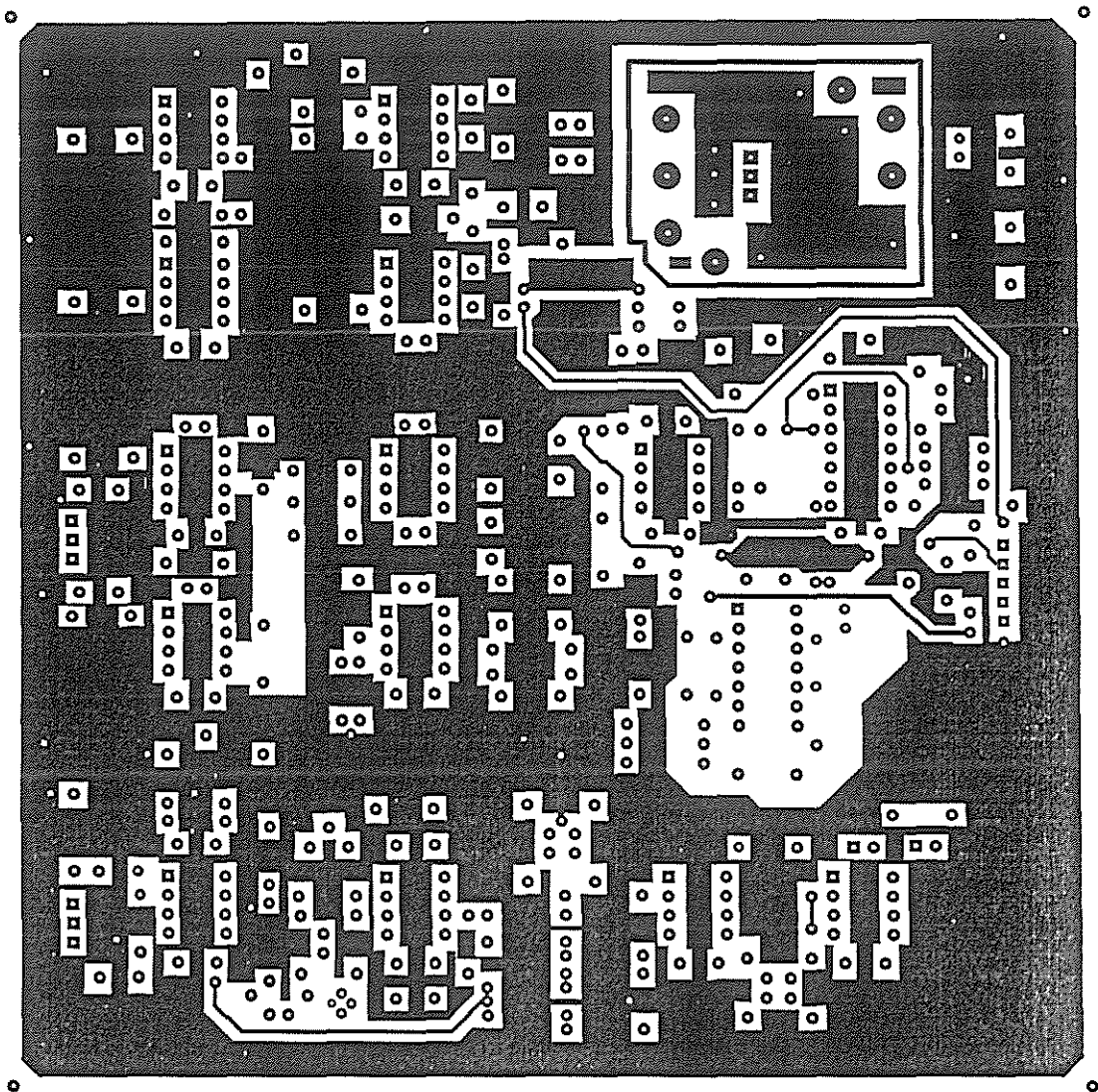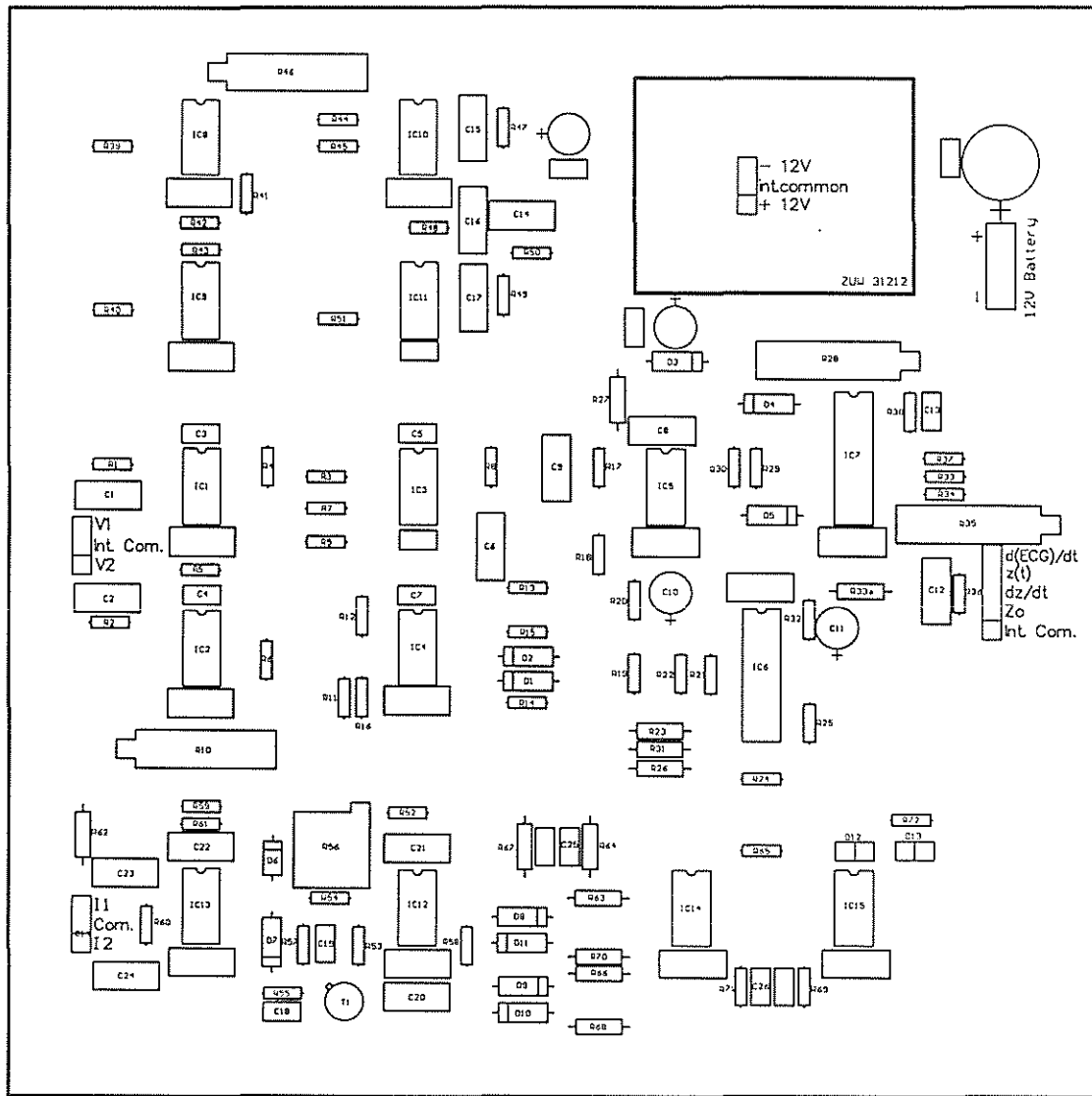
PCB layout of thorax simulator circuit
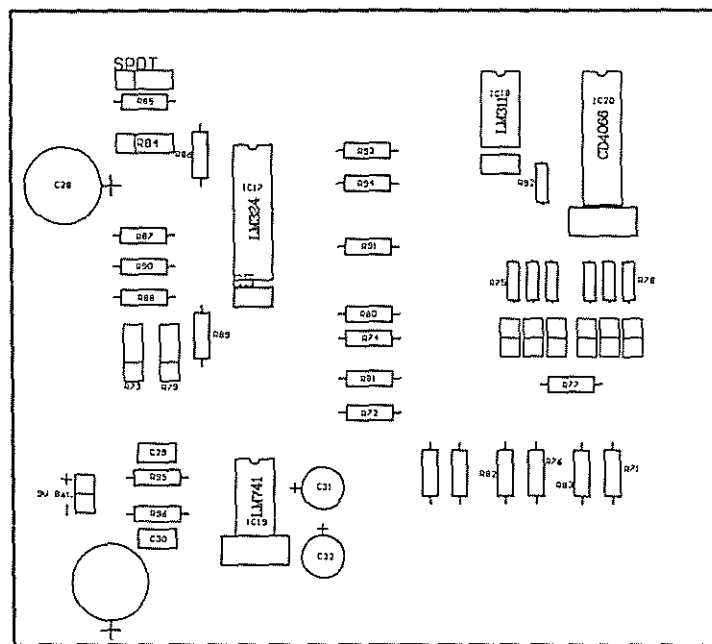
Component layout for simulator

PCB layout of solder side of ICG circuit

PCB layout of component side of ICG circuit

Component layout of ICG circuit

# REFERENCES

1. A.C.Guyton, *Textbook of Medical Physiology.* 7$^{th}$ ed. Philadelphia: Saunders, 1986.

2. T.C.Ruch and H.D.Patton, *Physiology and Biophysics.* Philadelphia: Saunders, 1965.

3. L.A.Geddes and L.E.Baker, *Principles of Applied Biomedical Instrumentation.* New York:Wiley, 1975.

4. L.E.Baker, "Principles of Impedance Technique". *IEEE Engg. in Medical and Biological Magazine,* 8(1), 1989, pp. 11-15.

5. R.P.Patterson, "Fundamentals of Impedance Cardiography.", *IEEE Engg. in Medical and Biological Magazine,* March 1989, pp. 35-38.

6. S.N.Mohapatra, "Impedance Cardiography" in J.G.Webster(ed.), *Encyclopedia of Medical Devices and Instrumentation.* Vol.3, New York: Wiley, 1992, pp. 1622-1632.

7. J.G.Webster, *Medical Instrumentation–Application and Design.* 2nd ed., Boston: Houghton Mifflin, 1998.

8. M.Qu, Y.Zhang, J.G.Webster, W.J.Tompkins, "Motion artifacts from spot and band electrodes during Impedance Cardiography." *IEEE Trans. on Biomed. Engg.*, Nov. 1986, Vol.33, pp. 1029-1036.

9. D.V.Nagvenkar, "Design and development of an impedance cardiograph", *B.Tech Project Report,* Dept. of Elect. Engg., IIT Bombay, April 1991.

10. H.Lakdawalla, " Electrode placement in impedance cardiography", *M. Tech seminar report,* Dept. of Elect. Engg., IIT Bombay, Oct. 1993.

11. S.M.Joshi, H.Lakdawalla, M.Ingle, "A Cardiac Output Monitor", *IRCC Funded Project Report,* Dept. of Elect. Engg., IIT Bombay, July 1994.

12. S.M.Joshi, "A cardiac Output Monitor", *B Tech. Project Report,* Electrical Engg. Dept., IIT Bombay, April 1993.

13. K.S.Patwardhan, "An Impedance Cardiography for stress testing." *M Tech Dissertation,* Dept. of Elect. Engg., IIT Bombay, Jan. 1997.

14. P.C.Pandey, "Contact impedance indicator," *Personnel Communication*. Dept of Electrical Engg., IIT Bombay, Nov.1999.

15. H.G.Goovaerts, "An electrically isolated balanced wideband current source: basic considerations and design", *Medical & Biological Engg. & Computing,* Sept.1998, pp. 598-603.

16. RCA Guide, *Linear Integrated Circuits*, pp. 286-291, 1992.

17 Linear Databook 2, *National Semiconductor Corporation*, pp. 2-40 to 2-45, 1988.

18. M.L.Meade, *Lock-in amplifiers: Principles and Application*", London: Peter Peregrinus, 1983.

19. COSEL 1998/1999, *Power Supplies Catalog*, Toyama: Cosel Ver 2.1 S, pp. 410-411.